RESPONSE OF VERTICALLY LOADED ENERGY PILES UNDER EARTHQUAKE EXCITATION

A Thesis Submitted to
the Graduate School of
İzmir Institute of Technology
in Partial Fulfilment of the Requirements for Degree of

MASTER OF SCIENCE

In Civil Engineering

by
Mehmet Göktuğ İNAYET

December 2023
İZMİR

We approve the thesis of **Mehmet Göktuğ İNAYET**

Examining Committee Members:

Prof. Dr. Alper SEZER
Department of Civil Engineering, Ege University

Assoc. Prof. Gürsoy TURAN
Department of Civil Engineering, İzmir Institute of Technology

Assist. Prof. Volkan İŞBUĞA
Department of Civil Engineering, İzmir Institute of Technology

8 December 2023

Assist. Prof. Volkan İŞBUĞA
Supervisor, Department of Civil Engineering, İzmir Institute of Technology

Prof. Dr. Cemalettin DÖNMEZ
Head of the Department of Civil Engineering

Prof. Dr. Mehtap EANES
Dean of the Graduate School

ACKNOWLEDGEMENTS

I would like to express my gratitude to my advisor Assist. Prof. Volkan İŞBUĞA for giving me a chance to work with him in this subject. His support, patience and guidance helped me to complete the thesis.

I would like to thank my thesis committee members Prof. Dr. Alper SEZER and Assoc. Prof. Gürsoy TURAN for their worthwhile comments and suggestions.

I am very grateful to my parents, Alimcan and Ayşegül İNAYET, my sister, Zeynep Göksu İNAYET and my brother, Mustafa Altuğ İNAYET for their love, support and encouragement. I would also like to thank my aunt, Hatice Kübra GÜLER for her assistance in difficult times.

I would also like to thank to Scientific and Technological Research Council of Turkey (TÜBİTAK) for their financial support in scope of 2210-A National MSc/MA Scholarship Program (Grant No: TÜBİTAK BİDEB 2210-A 2022/1 1649B022200830).

ABSTRACT

RESPONSE OF VERTICALLY LOADED ENERGY PILES UNDER EARTHQUAKE EXCITATION

Pile foundations are deep foundation systems that are used to transfer loads from superstructure to soil by either resisting surface friction or reaching a deeper and stiffer soil layer when geotechnical properties of the soil site are not sufficient to carry the loads transferred from superstructure. Energy piles fulfill the same function along with the ground heat exchanging via heat pump systems, thus satisfying the energy demand of a building for heating-cooling operations. This feature of energy piles draws attention as an innovative system supplying a renewable energy resource. However, heat exchanging operations of energy piles cause temperature variations on pile and the surrounding soil which may cause additional load and deformations. Moreover, temperature variations may affect the elasticity modulus of soils and shear strength of cohesive soils. In this study, earthquake response of an axially energy loaded pile was investigated considering the heating effect under 2020 Izmir earthquake motion using finite element method and compared to the those of identical regular piles. We performed analyses with different soil types, geometric properties, and temperature magnitudes under steady-state heating. Based on the analysis results, heating effect on pile head stiffness with respect to geometric properties were obtained. Two important conclusions have been made; (i) the most critical effect on heating depends on mechanical loading condition of pile and thermal expansion coefficient of soil, (ii) geometric properties may affect the temperature distribution resulting in an unforeseen change in pile head stiffness.

ÖZET

DÜŞEY YÜKLÜ ENERJİ KAZIKLARININ DEPREM HAREKETİ ALTINDAKİ TEPKİSİ

Kazık temeller sahadaki zeminin geoteknik parametreleri üst yapıdan aktarılan yükleri taşımak için yeterli olmadığında, yükleri yüzey sürtünmesi yoluyla veya daha derindeki sert zemin katmanlarına ulaşarak aktaran derin temel sistemleridir. Enerji kazıkları ise yük taşıma görevinin yanı sıra ısı pompası sistemleri aracılığıyla zeminle ısı alışverişi sağlar, böylelikle elde edilen ısı binanın ısıtma-soğutma ihtiyacını karşılar. Enerji kazıklarının bu özelliği, yenilenebilir bir enerji kaynağı sağlayan yenilikçi bir sistem olarak dikkatleri üzerine çekmiştir. Ancak enerji kazıklarının işlemleri sırasında kazıkta ve kazık çevresindeki zeminde sıcaklık değişimleri olur, bu da zemin ve kazıkta ek yük ve deformasyonlara sebebiyet verebilir. Ayrıca zeminin elastisite modülü ve kohezyonlu zeminlerin kesme dayanımı sıcaklık değişimlerinden etkilenebilir. Bu çalışmada sonlu elemanlar yöntemiyle ısıtma etkileri dikkate alınarak oluşturulan eksenel yüklü bir enerji kazığı modelinin 2020 İzmir deprem hareketi altındaki tepkisi incelenmiş ve aynı özelliklere sahip sıradan bir kazığın deprem tepkisiyle karşılaştırılmıştır. İncelemeler farklı zemin türleri, geometrik özellikler ve sıcaklık değerleri ile kararlı durum ısıtma altında yapılmıştır. Analiz sonuçlarına dayanarak ısıtmanın geometrik özellikler açısından kazık baş rijitlik eğrisine etkisi elde edilmiştir. İki önemli bulgu bulunmuştur; (i) ısıtmanın en kritik etkisi kazığın mekanik yüklenme koşuluna ve zeminin ısıl genleşme katsayısına bağlıdır, (ii) geometrik özellikler sıcaklık dağılımını etkileyerek kazık baş rijitliğinde öngörülemeyen değişimlere sebep olabilir.

TABLE OF CONTENTS

LIST OF FIGURES

Figure **Page**

Figure **Page**

Figure **Page**

LIST OF TABLES

Table **Page**

CHAPTER 1

INTRODUCTION

Sustainability has a significant importance in engineering applications since engineering applications affect the world in terms of environment, consumption of resources, and cost. These impacts are vital for the life quality and the future of the world. Hence, sustainability criteria aim to protect the world by minimizing the impacts of engineering applications while maintaining the functional quality of engineering products.

Many studies have been conducted on sustainability in search of sustainable developments. The use of renewable energy sources is presented as one of the solutions towards a more sustainable future. Renewable energy sources are excellent solutions for minimizing the consumption of resources, environmental impacts, and cost while meeting the energy requirement efficiently. Benefits of renewable energy sources made it an interesting subject for many disciplines including civil engineering.

Geothermal energy utilizes heat energy obtained from underground resources. In 1980s, energy foundations have been developed which are used for both load-bearing and heat exchanging from ground via heat pump systems (Brandl, 2006). Heat energy obtained by energy foundations are used in heating-cooling process of the superstructure. The first applications on the basis of energy foundations were made in Switzerland, Austria, England, and Germany, and these countries were pioneers in this field (Bouazza et al., 2011). Geothermal energy potential is high in various regions of our country, such as Aydın, and geothermal systems are widely used in these regions to obtain geothermal energy (https://www.mta.gov.tr/v3.0/sayfalar/hizmetler/jeotermal-harita/images/3.jpg). However, the share of energy foundations in these systems is negligible. The widespread use of energy foundations in Turkey should be encouraged because through these structures, long-term problems in terms of cost, environment, and consumption of resources can be avoided.

The most common energy foundation type is energy pile, which is a type of deep foundation reaching great depths below ground. Benefits of the energy piles can be summarized in general in three topics, emphasized by many researchers, as follows:

energy efficiency (Brandl, 2006), cost efficiency (Brandl, 2006), and reduction of CO_2 emissions due to the heating-cooling process of a building (Laloui et al., 2006; Amis and Loveridge, 2014).

The significant problem regarding the use and the design of the energy piles is that the heating-cooling problem causes a temperature variation in the surrounding soil, which in turn, influences its material properties.

Temperature variations cause thermal volume changes in materials. The material expands as it heats up and contracts as it cools. In this case, the pile and the ground are exposed to additional loads and deformations caused by temperature variations (Bourne-Webb et al., 2009). Moreover, other thermally induced effects are anticipated by many researchers, such as an increase in creep effect and irreversible displacements in the long term (Akrouch et al., 2014), and changes in some engineering properties of soils (Mitchell, 1969). Two critical material parameters which can alter the response of the pile, are the Young's modulus (Murayama, 1969; Mitchell, 1969; Arzanfudi et al., 2020; Heidari et al., 2022) and cohesion (Laguros, 1969; Mitchell, 1969; Heidari et al., 2022) since they are directly related to the stiffness and strength of the soil. Findings of Laguros (1969) proved that cohesion increases with temperature rise. Young's modulus of soil decreases with temperature increase based on the findings of Murayama (1969). Numerous studies have been conducted in the literature on the thermo-mechanical behavior of soils and energy piles. However, temperature effects on Young's modulus and cohesion have not been considered in most of the studies. Arzanfudi et al. (2020) considered a temperature dependent elasticity for freezing and thawing in porous media domains. Heidari et al. (2022) considered temperature-dependent cohesion and elasticity modulus by formulating the findings of Laguros (1969) and Murayama (1969) for laterally loaded energy piles under steady-state heat transfer conditions.

Although the literature on energy foundations is vast, the response of the energy foundations in earthquake-prone regions has not been studied. Lack of information regarding the response of the energy piles under earthquake motions can lead to uncertainties in the use and design of such foundation types in earthquake-prone regions. This study aims to investigate the response of energy pile foundations under earthquake motion and compare them to those of regular piles. Thus, an insight into the applicability of energy piles placed in seismic zones can be obtained.

CHAPTER 2

LITERATURE REVIEW

2.1. Energy Piles

Piles are deep foundations, which are commonly used when the geotechnical properties of soils are not sufficient to resist the loads transferred from the superstructure. Hence, piles reach great depths either to transfer the loads to deeper and stiffer soil/rock layers or to resist the loads by means of side friction. Energy piles fulfill the same purpose and are used as a heat source for the superstructure. Heat transfer from the ground is possible based on the constant temperature profile of the soil below a certain depth. Ground temperature profile visualized by Brandl (2006) is demonstrated in Figure 2.1.

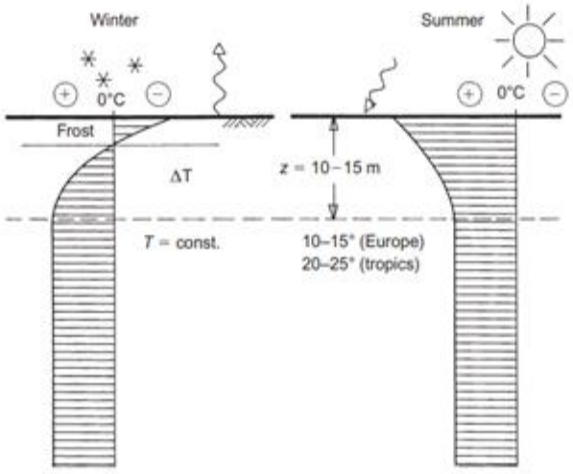

Figure 2.1. Seasonal ground temperature profile for Europe and tropics (Source: Brandl, 2006)

As seen in the figure, ground temperature varies depending on the ambient temperature up to a certain depth (10-15 m). Brandl (2006) states that when this depth is exceeded, the temperature remains almost constant throughout the year. The researcher also notes that this temperature may vary according to the region, for example, it can reach 10-15^{o}C in Europe and 25^{o}C in the tropics. Then, the constant temperature can be used as a heat source or heat sink (Brandl, 2006).

Figure 2.2 and Figure 2.3 are shown to visualize the ground heat exchanging procedure (Laloui and Di Donna, 2011; Abuel-Naga et al., 2015).

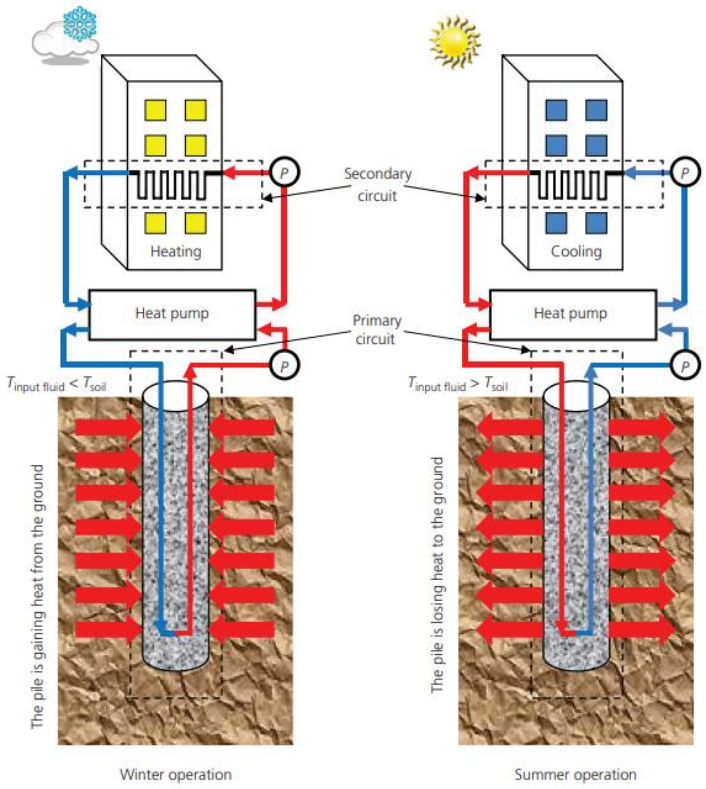

Figure 2.2. Basic scheme of energy pile system in winter and summer (Source: Abuel-Naga et al., 2015)

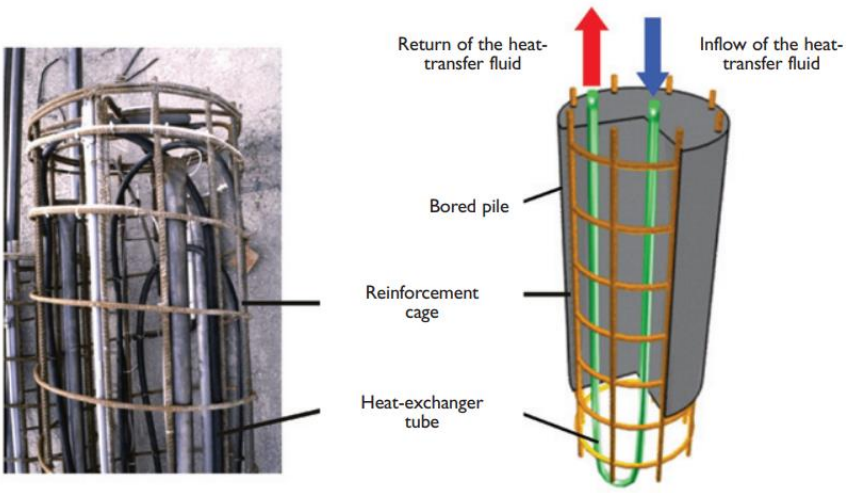

Figure 2.3. Interior of an energy pile (Source: Laloui and Di Donna, 2011)

The workflow of the energy piles is explained by Brandl (2006) as follows: Energy pile system consists of three basic components; primary circuit, heat pump, and

secondary circuit as shown in Figure 2.2. The primary circuit is the energy pile equipped with closed coils of heat exchanger pipes as shown in Figure 2.3. Heat exchanger pipes made of high-density polyethylene are attached inside the reinforcement cage of the pile. The pipes are connected to a heat pump system called a ground source heat pump (GSHP) system in ground heat exchange. A heat-transferring fluid is circulated through the pipe from the GSHP at a certain temperature in order to maintain the desired heat flow corresponding to heating or cooling process. The temperature of the inlet fluid must be lower than the temperature of the soil in order to be used in heating during winter ($T_{pile}<T_{soil}$). On the other hand, the temperature of the inlet fluid is higher than the temperature of the soil for cooling the building in summer ($T_{pile}>T_{soil}$). Heat is transferred from the outlet pipe of the primary circuit to the GSHP and, consequently, to the secondary circuit, which is the distribution network of the building for heating and cooling.

Benefits of the energy piles are reported by many researchers in terms of energy efficiency, cost efficiency and reduction of CO_2 emissions caused by heating-cooling system of a building (Brandl, 2006; Laloui et al., 2006; Martin et al., 2010; Amis and Loveridge, 2014). Brandl (2006) provided a graph demonstrating the annual energy demand and output of a building using energy pile system. The graph is presented in Figure 2.4.

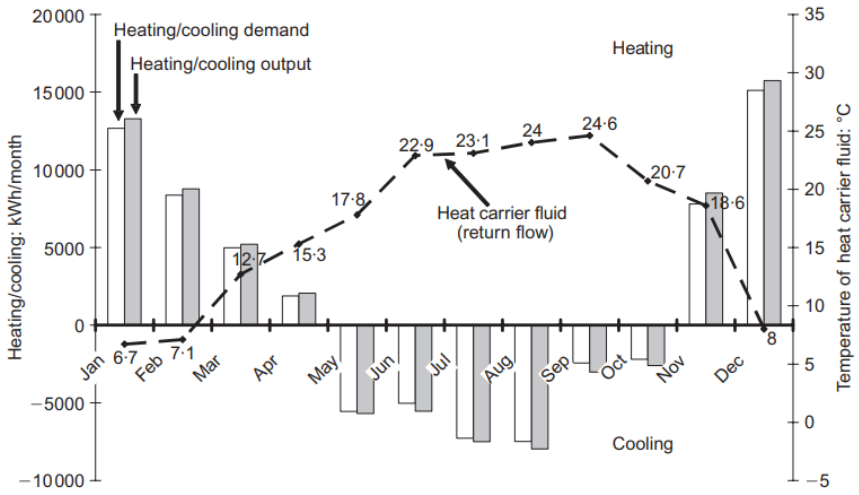

Figure 2.4. Annual energy demand of a building and energy output of energy piles, temperature of heat carrier fluid is also shown. (Source: Brandl, 2006)

Figure 2.4 indicates that the energy piles are efficient in supplying energy to the heating-cooling system of a building as the energy output is greater than the energy demand.

Amis and Loveridge (2014) shared data relating to the number of energy pile installations in the UK and corresponding annual CO_2 savings due to heating-cooling operations. The data is demonstrated in Figure 2.5.

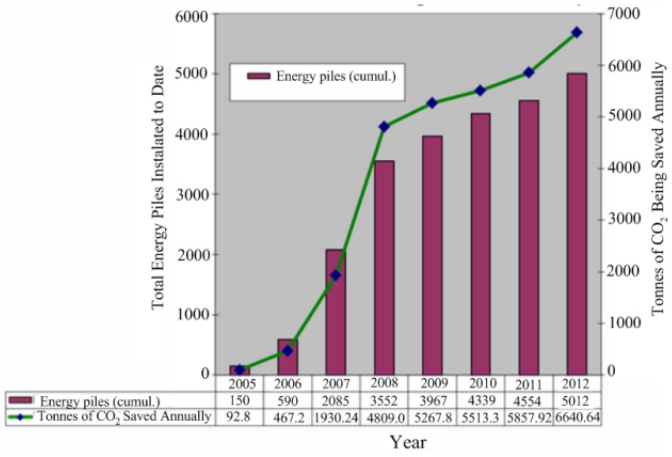

	2005	2006	2007	2008	2009	2010	2011	2012
Energy piles (cumul.)	150	590	2085	3552	3967	4339	4554	5012
Tonnes of CO_2 Saved Annually	92.8	467.2	1930.24	4809.0	5267.8	5513.3	5857.92	6640.64

Figure 2.5. Energy pile installations in UK and corresponding annual CO_2 savings (Source: Amis and Loveridge, 2014)

From Figure 2.5, it can be seen that the increase in energy pile installations in UK increased the annual CO_2 savings. Therefore, it can be concluded that as the energy pile systems have become more prevalent, environmental impacts due to heating-cooling operations can be reduced significantly.

2.2. Temperature Effects on Soil Properties

Investigation of the effects of temperature on soil behavior has a vital importance in cases where the soil is constantly exposed to temperature variations. Extreme weather conditions may cause freezing-thawing on the ground exposed to the atmosphere or engineering applications such as nuclear facilities and geothermal systems exposing the soil to high thermal cycles. Such thermal actions may alter the soil properties, such as strength and stiffness, which may pose a risk to the safety of the structure. Due to its

significance, the temperature effects on soil behaviour have been studied by various researchers.

Campanella and Mitchell (1968) conducted drained and undrained Triaxial tests on saturated clays and observed that an increase in temperature causes an increase in pore water pressure in undrained conditions and an additional volume change in drained conditions. The most important reason for this is the thermal expansion of water and the compressibility of soils. In drained conditions, volume can change freely due to temperature increase, whereas in undrained conditions, pore water pressure increases since thermally expanded water is not allowed to drain.

Laguros (1969) studied the effects of temperature on clayey soils and observed that the unconfined compressive strength increased as temperature increased. From the unconfined compressive strength, the relationship between undrained shear strength/cohesion and temperature can be determined. The formula for this relationship was derived by Heidari et al. (2022) in Equation 2.1:

$$c_{u(T)} = 0.53\Delta T + c_{u,0} \tag{2.1}$$

where $c_{u(T)}$ is cohesion at a specific temperature (kPa), $c_{u,0}$ is cohesion at a reference (initial) temperature (kPa), and ΔT is temperature change (^{o}C).

Murayama (1969) studied the effect of temperature changes on the modulus of elasticity on clayey soils. It has been observed that the increase in temperature decreases the Young's (elasticity) modulus, and the relationship between them is shown in Equation 2.2 by Heidari et al. (2022):

$$E_{s\,(T)} = E_{s,0} - 0.39\Delta T \tag{2.2}$$

where $E_{s\,(T)}$ is the elasticity modulus of soil at a specific temperature (MPa), and $E_{s,0}$ is the elasticity modulus of soil at a reference (initial) temperature (MPa).

Heidari et al. (2022) assumed that temperature-dependent soil elastic modulus is valid for both sandy and clayey soils, whereas temperature-dependent cohesion is only valid for clayey soils.

Arzanfudi and Al-Khoury (2018) formulated a temperature-dependent elasticity modulus of soils, which is valid under freeze-thawing conditions:

$$E_{s\,(T)} = E_{s,0}\, e^{-b(T_s - T_0)} \tag{2.3}$$

where T_s is the temperature of the solid matrix (°C), T_0 is the reference (initial) temperature (°C), and b is a material parameter (1/°C).

Arzanfudi et al. (2020) used this formulation for modeling energy pile operations in which input temperature varies from -6 to 40 °C and reported b=0.1 for sandy gravel and London clay. The Equation can be used for energy pile operations where soil temperature reaches below 0 °C.

Temperature dependency of friction angle is not clear in the literature as the findings of various studies are contradictory. For example, the findings of Yavari et al. (2016) indicated that upon heating, friction angle decreases up to a certain temperature and remains constant afterward or increases up to a certain temperature and decreases afterward. Moreover, the variations in friction angle under temperature increase were found to be very slight. In the investigations on thermo-mechanical modeling of energy piles, it is commonly accepted that the friction angle of soils does not vary with temperature (Laloui et al., 2006; Saggu and Chakraborty, 2015; Heidari et al., 2022). Hence, the assumption of a temperature-independent friction angle is made in this thesis.

Studies on the behavior of clayey soils under the effects of temperature are more common in literature. Laloui (2001) investigated the thermo-mechanical behavior of soils by developing a constitutive model based on experimental data. Laloui (2001) emphasized that the heating effect in clayey soils significantly changes the clay texture, thus creating the most important thermal characteristic of the clay. For example, while it is known that an increase in temperature will expand the materials, it has been observed that normal consolidated clayey soils contract under heating and expand under cooling. This behavior was attributed to the effect of overconsolidation ratio (OCR), soil type, and soil plasticity. Laloui (2001) claimed that clayey soils subjected to heat cycles go through a process called thermal hardening, and normally consolidated clays behave like overconsolidated clays. Moreover, it has been found that the deformation caused by heating cannot be completely reversed under cooling. He found that under cyclic loads, the heated samples were subjected to smaller strains, and the excess pore water pressure was higher in the unheated samples. Later, the model was improved by many researchers

(Laloui and Cekerevac, 2008; François and Laloui, 2008; Laloui and François, 2009; Di Donna and Laloui, 2015).

Cekerevac and Laloui (2004) examined the effects of temperature on Kaolin clay. They found that (i) the shear strength increases as the temperature increases, but the material exhibits a brittle behavior, (ii) thermal volume changes depend on the over-consolidation ratio (OCR), (iii) the yield limit decreases as the temperature increases, (iv) the pre-consolidation pressure decreases as the temperature increases and (v) initial elastic modulus increases with increasing temperature.

Abuel-Naga et al. (2007) investigated the effect of temperature variations on shear strength of soft Bangkok clay by direct heating and exposing the samples to heat cycles. They concluded that, as the temperature increases, (i) stiffness, drained and undrained shear strengths increase, (ii) plastic strain rate increases, and (iii) as the over-consolidation ratio (OCR) increases, the amount of contraction due to temperature decreases and it exhibits expansion behavior after exceeding a certain value.

Cekerevac and Laloui (2010) studied the cyclic behavior of Kaolin clay under high temperatures. As a result, they determined that the heated samples behaved as a denser material than the unheated samples and increased their resistance to shear cycles. Thus, they suggested that the application of thermal pretreatment to cohesive soils could increase earthquake resistance.

While the studies on the thermo-mechanical behavior of clays are vast, only a few studies have investigated the effects of temperature on sandy soils (Yavari et al., 2016). The lack of research in the field creates a misconception that the elastic modulus of sand does not change with respect to temperature variations. The elastic modulus of a material is expected to decrease with increasing temperature. Hence, assuming a temperature-dependent elastic modulus for sandy soils would be valid. For this study, the assumption of Heidari et al. (2022) for temperature-dependent sand elastic modulus is considered to be valid.

Lastly, one of the most important temperature-dependent properties is the coefficient of thermal expansion (α), which affects the thermo-mechanical behavior of both concrete and soils. The coefficient of thermal expansion represents the expansion and contraction behavior of materials under temperature variations. This value can be obtained from laboratory and in-situ experiments as well as the assigned values in the standards can be used. For example, the thermal expansion coefficient of concrete was assigned as $10^{-5}/^{o}C$ in BS EN 1991-1-5:2003. Thermal expansion can affect the thermo-

mechanical behavior of energy piles in terms of load-bearing capacity, shaft resistance, and strength of concrete. Detailed information on the thermo-mechanical response of energy piles will be discussed in the following section.

2.3. Modeling of Energy Piles

Numerical modeling of energy piles requires the coupling of thermal and mechanical analysis, which combines the heat transfer analysis to obtain the temperature field throughout the domain and the static analysis to observe the temperature effect on the mechanical response. Abaqus provides a fully coupled temperature-displacement analysis, which performs heat transfer analysis and the consequent mechanical response at the same time. Firstly, it is compulsory to understand the heat transfer mechanism of energy piles in order to construct a successful energy pile model. Figure 2.6 shows the heat transfer mechanism of soils due to energy pile operations.

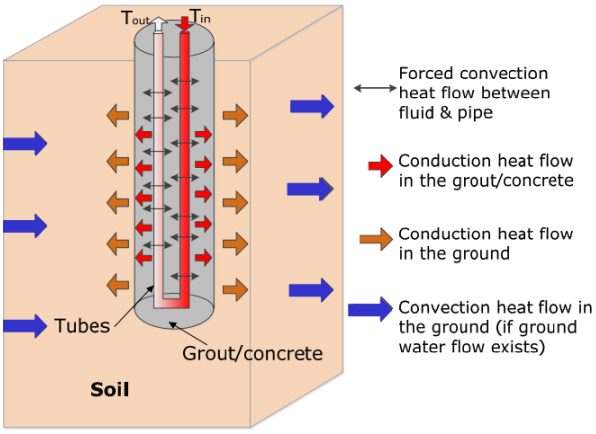

Figure 2.6. Heat transfer mechanism of energy piles (Source: Martin et al., 2010)

Figure 2.6 shows that the heat transfer modes include forced convection between the pipe and the fluid, conductive heat transfer in concrete, conductive heat transfer in soil, and convective heat transfer due to groundwater flow if a groundwater table exists.

In order to simplify the heat transfer mechanism of energy piles, various researchers assumed a uniform temperature change along the pile body (Laloui et al., 2006; Saggu and Chakraborty, 2015; Salciarini et al., 2015; Bourne-Webb et al., 2016; Heidari et al., 2022). Moreover, the temperature of the ground surface is commonly

assumed to be constant and equal to the ambient soil temperature which means the air temperature is assumed to be the same as the soil temperature (Laloui et al., 2006; Saggu and Chakraborty, 2015; Salciarini et al., 2015; Wang et al., 2015). Exceptions are also made by many researchers, which ground surface temperature is not equal to the ambient soil temperature (Bourne-Webb et al., 2016), and the ground temperature is adiabatic, which means heat flux is not allowed on the ground surface thus atmospheric effects are not considered (Rotta Loria and Laloui, 2016; Heidari et al., 2022).

Modeling the heat exchange between the energy pile and soil requires determination of thermal parameters. The thermal parameters are thermal conductivity (λ), which represents the heat transfer due to the contact of the materials and specific heat capacity (c_s), which is a measure of heat energy required to increase the temperature of the material. The distribution of the temperature profile in pile and soil under temperature effects depends on these thermal properties. These parameters can be obtained by experimental methods. There are a number of works reporting such parameters in the literature depending on the soil structure (Marshall, 1972; Farouki, 1981; Rees et al., 2000; Abu-Hamdeh, 2003; Hamdhan and Clarke, 2010; Aliberdi-Pagola et al., 2017).

Heat transfer analysis of energy piles is commonly performed under transient conditions (Laloui et al., 2006; Olgun et al., 2014; Saggu and Chakraborty, 2015; Salciarini et al. 2015; Wang et al., 2015). However, steady-state heat transfer analyses are made by various researchers for the numerical modeling of energy piles (Bourne-Webb et al., 2016; Rotta Loria and Laloui, 2016; Heidari et al., 2022). Investigation of the thermo-mechanical response of energy piles is crucial since structural risks are present. There are numerous studies which investigated the thermo-mechanical response of energy piles (Laloui et al., 2006; Bourne-Webb et al., 2009; Peron et al., 2011; Amatya et al., 2012; Olgun et al., 2014; Saggu and Chakraborty, 2015; Suryatriyastuti et al.,2013, 2015; Arzanfudi et al., 2020; Heidari et al., 2022).

In order to investigate the additional loads caused by temperature variations, Laloui et al. (2006) conducted field measurements where an energy pile was installed, and a numerical analysis was conducted and compared with experimental data. Researchers used a coupled thermo-hydro-mechanical model in numerical analysis and concluded that their approach to numerical analysis matched with the experimental data. Based on their results, an uplift on the pile head was observed for energy piles, which are only subjected to thermal loads, whereas an increase in compressive stress on the pile toe was observed. Results on energy piles subjected to mechanical and thermal loads

indicated that at a distance of 1 m from the pile, the effect of the mechanical load was negligible, and the effect of the thermal load was more dominant; consequently, the change in effective stress and pore-water pressure was negligible.

Bourne-Webb et al. (2009) investigated the effect of thermal cycles on energy piles via field measurements conducted on an energy pile foundation in London clay, and the findings were explained by a simplified mechanism. This simplified mechanism is demonstrated in Figure 2.7.

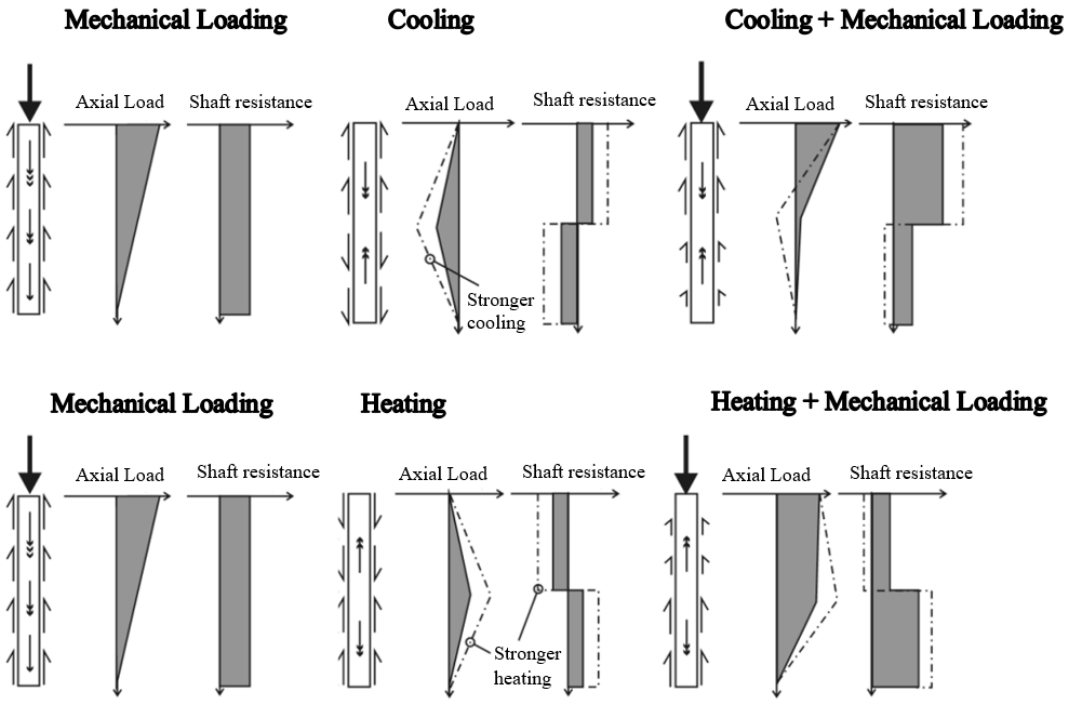

Figure 2.7. Axial load distribution on the energy pile under heating-cooling effects (adopted from: Bourne-Webb et al., 2009)

As it can be seen in the figure, heating increases the compressive stresses on the pile, whereas cooling reduces the compression. Tensile stresses may occur on the pile after a certain depth upon more substantial cooling.

Amatya et al. (2012) investigated the thermo-mechanical behavior of energy piles by combining the results of different field measurements. In this context, axial load and shaft resistance results obtained from three different fields were examined. The effects of thermal and thermo-mechanical loads on axial load and shaft resistance are explained based on the measurements. According to the researchers, (i) mobilized shaft resistance of mechanically loaded energy piles is greatly affected by temperature variations, (ii) thermally induced shaft resistance is greater in stiff clayey/silty soils than soft clays and

(iii) heating-cooling cycles do not harm the building; however, differential settlements in energy pile groups should also be given separate consideration.

Olgun et al. (2014) examined the effects of radial expansion on the pile-soil interaction. As a result of the analysis made with the finite element method, it has been determined that the radial expansions under heating will not significantly increase the load-bearing capacity of the pile.

In finite element analysis, the pile is generally considered linear elastic (Laloui et al., 2006; Hussein and Albusoda, 2021; Heidari et al., 2022). However, Saggu and Chakraborty (2015) defined the concrete damage plasticity model as pile behavior in their finite element model. Thus, deformations caused by thermo-mechanical loads reduce the strength of concrete. Saggu and Chakraborty (2015) modeled energy piles using thermal parameters and heating-cooling load used by Laloui et al. (2006), soil parameters used by Das (2013) and concrete damage plasticity values used by Tiwari et al. (2012). Laloui et al. (2006) defined a temperature change of 21^{o}C and applied 12 days of heating and 16 days of cooling. Saggu and Chakraborty (2015) applied the same heat cycle by defining a 3-year period with different mechanical loads and pile types. Soil behavior was described by Laloui et al. (2006) with the Drucker-Prager model, while Saggu and Chakraborty (2015) modeled it with the Mohr-Coulomb model.

Heidari et al. (2022) investigated a static laterally loaded energy pile under steady-state heating conditions using both the analytical method and the finite element method. No vertical load was applied on the pile and the temperature variation was defined as $\Delta T = 0$ and $\pm 10^{o}$C. The adiabatic boundary was defined on the ground surface, which means heat flux is not allowed. Separate analyses were conducted with different lengths of pile caps, for clayey and sandy soils. The Mohr-Coulomb plasticity model was used including temperature-dependent elasticity modulus of soils and cohesion of clay. Based on the results, it was concluded that maximum lateral displacement and normalized internal moment under heating decreased in sandy soils and increased in clayey soils. The difference between the behavior of sand and clay may depend on the combination of various factors in their work, such as differences in temperature distribution, thermal expansion coefficient and soil elastic modulus.

Numerous studies can be found in the literature on the thermo-mechanical behavior of energy piles; however, not all aspects of energy piles have been enlightened, such as their earthquake response. The following section will cover the finite element modeling approach of piles under earthquake motion.

2.4. Finite Element Modeling of Earthquake Motion

Finite element modeling of earthquake motion requires the determination of damping and representing far-field regions using special boundaries. Earthquake motion is generally applied at the base of the model. Hussein and Albusoda (2021) modeled the earthquake response of a pile by applying the acceleration-time history of 1995 Kobe earthquake to the base of the model. Their approach was to match the numerical results with the experimental results. The model was composed of two soil layers and a combined laterally and vertically loaded pile. The soil was modeled using Mohr-Coulomb plasticity and infinite elements were introduced by extending the model domain at the two ends of the model in the *x*-direction to simulate the quiet boundary behavior during earthquake motion. Infinite elements and quiet boundary condition are based on the works of Zienkiewicz et al. (1983) for static loading and Lysmer and Kuhlemeyer (1969) for dynamic loading. The quiet boundary behavior represents an unbounded field, that is, a far-field region. In reality, the earthquake affects a very large area, but in the case of an analysis with the finite element method, the area of interest is very small compared to the actual site behavior. Infinite elements prevent wave reflections during earthquake motion. The size of the infinite element should be appropriately adjusted to fulfill its purpose. Figure 2.8 shows the appropriate size requirement for infinite elements.

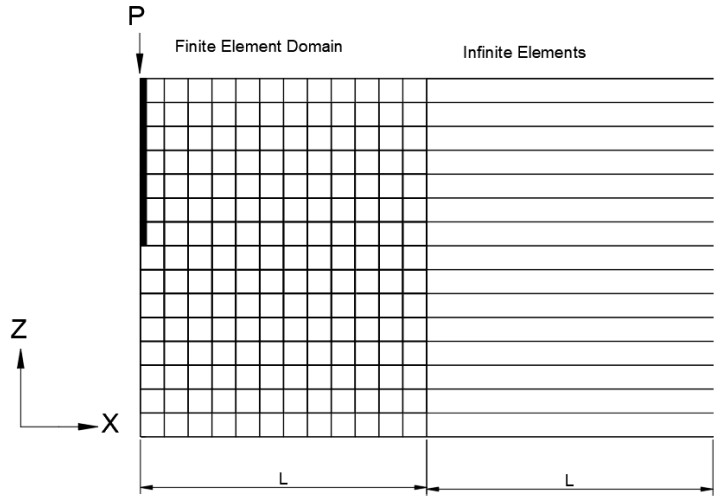

Figure 2.8. Infinite element size requirement based on the Abaqus User's Manual

Infinite elements are constructed by extending the boundaries on the direction of motion about half-length of the finite element domain based on the Abaqus User's Manual, as shown in Figure 2.8.

For soil damping during earthquake motion, Rayleigh damping coefficients are used and the coefficients (α) and (β) represent mass-proportional and stiffness-proportional damping, respectively. The following formulation represents the use of Rayleigh damping coefficients in the determination of damping behavior:

$$\xi = \frac{\alpha}{2w_i} + \frac{\beta w_i}{2} \tag{2.4}$$

where ξ is the damping ratio of soil (%), w_i is the predominant frequency of the i^{th} mode (rad/s).

Common practice is that the first mode is the natural frequency of the site soil, w_1 and the second mode is the predominant frequency of the input motion, w_2 (Hashash et al. 2010). Using a target damping ratio and the frequencies w_1 and w_2, Rayleigh damping coefficients can be determined. Hudson et al. (1994) defined a coefficient (n), which is rounded to the closest odd integer greater than w_2/w_1. Then, the second frequency is modified as follows:

$$(w_2)_{new} = n.w_1 \tag{2.5}$$

Modification of the second frequency was to prevent over-damping outside the frequency range (Hudson et al., 1994).

CHAPTER 3

METHODOLOGY

Modelling energy piles using Abaqus software requires multiple steps to simulate the exact sequence of loading conditions, starting from the application of mechanical loads to the last step of applying earthquake motion. For the entire analysis, it was assumed that the pile and soil were perfectly bonded. Steady-state heating was considered for energy piles with temperature increases of ΔT= +21°C and, ΔT= +30°C. The initial temperature, T_0=15°C was considered a reference temperature for temperature-dependent properties, such as thermal expansion coefficient (α), which means at T=15°C, behavior of energy pile and regular pile would be the same. The far-field region was represented by introducing infinite elements.

In order to investigate the earthquake response of energy piles, three-dimensional model geometry was constructed in Abaqus software. The geometry and boundary conditions of the model are shown in Figure 3.1.

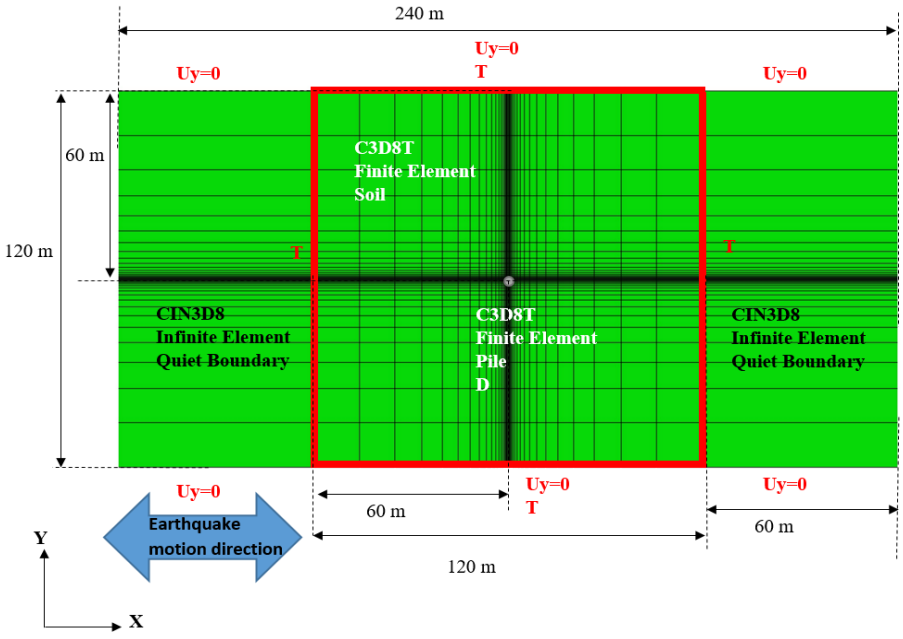

(a)

Figure 3.1. Model geometry and boundary conditions on (a) *XY* plane, (b) *YZ* plane

(cont. on next page)

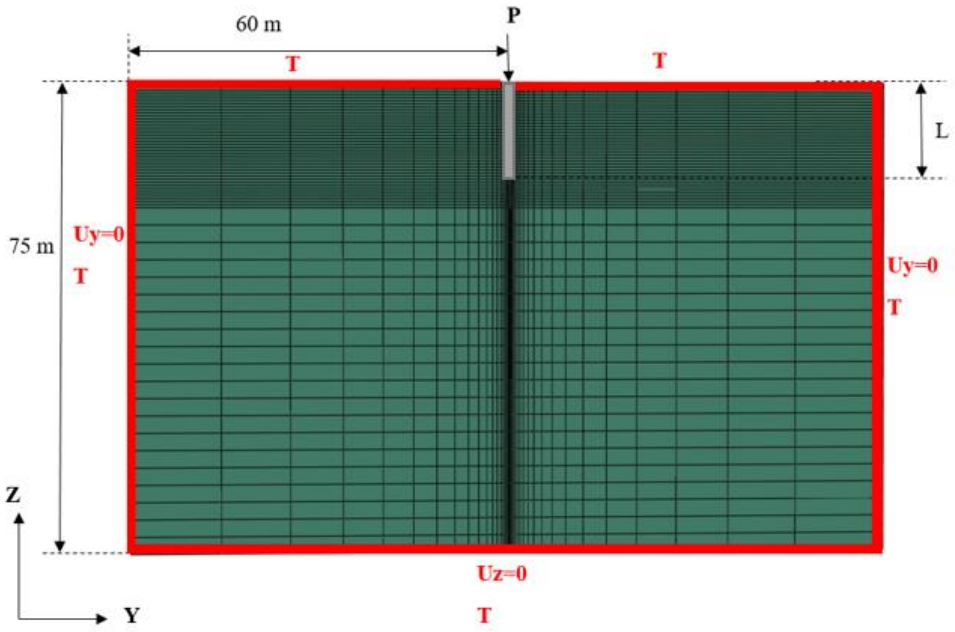

(b)

Figure 3.1 (cont.)

Figure 3.1 (a) demonstrates the top view in the *XY* plane of the model. The finite element domain has a size of 120x120 m in the *XY* plane. Infinite elements were constructed by extending the boundaries on the direction of motion about half-length (60 m) of the finite element domain, which satisfies the criterion for the size requirements of the infinite element, as demonstrated in Figure 2.8 in the previous chapter. Three-dimensional coupled displacement-temperature element formulation (C3D8T) in finite element domain and three-dimensional infinite element formulation (CIN3D8) were used. Boundaries on the *y*-face were not allowed to displace, whereas displacements on the *x*-direction were allowed. The reason is to allow the earthquake motion in the *x*-direction. Figure 3.1 (b) shows the side view in the *YZ* plane of the model, and it can be seen that the base of the model is not allowed to displace in the *z*-direction. Constant temperature boundary conditions (T=15^{o}C) representing ambient soil temperature are defined on the ground surface, sides of the finite element domain where the infinite elements start, and base of the model. Constant temperature boundary conditions must be defined in steady-state heating; otherwise, the field would act as an "infinite heat reservoir" (Rotta Loria and Laloui, 2016).

The model was composed of a 75 m deep soil layer and an axially loaded pile with a diameter of *D* and length of *L* placed at the center of the domain. The axial load (*P*) applied to the pile was 500 kN. The effect of different *L/D* ratios was investigated where:

- *L/D*=15; D=1 m, L=15 m,
- *L/D*=30; D=0.5 m, L=15 m,
- *L/D*=40; D=0.5 m, L=20 m.

Table 3.1 shows the properties of materials used in the analyses. Piles placed in sand and clay soils were investigated, and The Mohr-Coulomb plasticity model was used with temperature-dependent cohesion (Equation 2.1) defined for clay and temperature-dependent elastic modulus (Equation 2.2) defined for both soil types. In our analyses, the mechanical properties of soils were selected from Das (2013). Then, the mechanical properties of concrete and thermal properties of concrete and sand were taken from the study of Saggu and Chakraborty (2015), while the thermal properties of clay were taken from Arzanfudi et al. (2020).

Table 3.1. Material properties used in the analysis (Das, 2013; Saggu and Chakraborty, 2015; Arzanfudi et al., 2020)

Parameter	**Sand**	**Clay**	**Pile**
Density, ρ (kg/m^3)	1733	1733	2500
Young's modulus, E_0 (Pa)	$15x10^6$	$15x10^6$	$27.38x10^9$
Poisson's ratio, ν	0.3	0.3	0.2
Cohesion, c (Pa)	500	20,000	-
Friction angle, φ (^{o})	30	20	-
Dilation angle, ψ (^{o})	1	1	-
Thermal conductivity, λ (W/m ^{o}C)	1.8	1.5	2.1
Thermal expansion coefficient, α (1/ ^{o}C)	10^{-4}	$1.5x10^{-5}$	10^{-5}
Specific heat capacity, c_S (J/kg ^{o}C)	1200	1500	800

For the input earthquake motion, the acceleration history of the 2020 Izmir Earthquake is obtained from TK3519 station (https://tadas.afad.gov.tr/). Figure 3.2 and Figure 3.3 shows the E-W and N-S records of the acceleration history of the 2020 Izmir Earthquake.

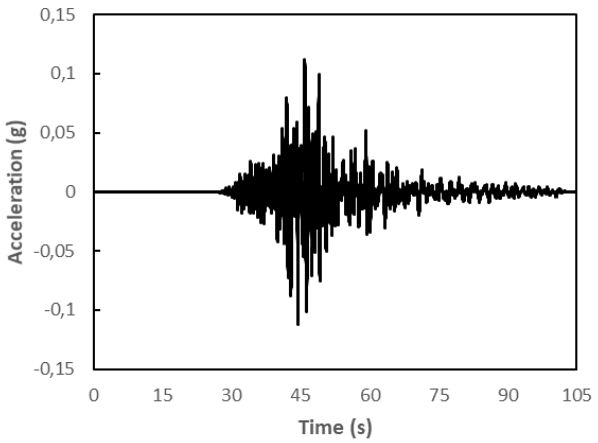

Figure 3.2. 2020 Izmir Earthquake acceleration-time history of TK3519 station E-W component (https://tadas.afad.gov.tr/)

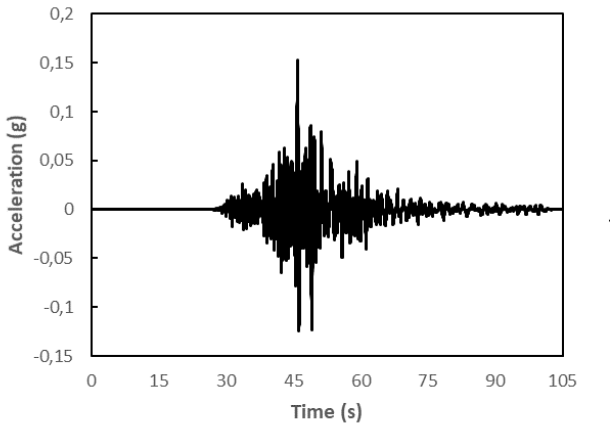

Figure 3.3. 2020 Izmir Earthquake acceleration-time history of TK3519 station N-S component (*https://tadas.afad.gov.tr/*)

The duration of the motion is 104.99 seconds for both records. Peak acceleration of N-S and E-W components are 0.153g and 0.112g, respectively. The N-S and E-W components were applied to the model in separate analyses, since it is not known which component will produce the maximum response.

Modeling earthquake response requires the definition of damping behavior. For this study, Rayleigh damping coefficients were determined by the following approach:

- The target damping ratio is assumed to be 5%.
- The natural frequency of the soil is where the earthquake motion is recorded (Kömeç Mutlu et al., 2023). The obtained frequency is accepted as target frequency 1, w_1=2.5 rad/s.

- The predominant period of earthquake motion for both N-S and E-W components are taken from the database provided by AFAD (https://tadas.afad.gov.tr/). Then, the predominant period is converted to predominant frequency which is used as target frequency 2. Predominant frequencies of E-W and N-S components are w_2=6.28 rad/s. w_2=6.58 rad/s.
- Equation 2.5 is applied and same *n* value (3) is determined for both N-S and E-W components. Thus, target frequencies are determined as w_2=7.5 rad/s.
- Consequently, substituting the target frequencies and damping ratio to the Equation (2.4) results in the determination of Rayleigh damping coefficients (α) and (β), which were calculated as α=0.188496 and β=0.009947.

Modeling of energy piles under earthquake motion using Abaqus software consisted of the following steps:

1. Initial step: Defining initial geostatic stress, initial temperature and mechanical boundary conditions
2. Geostatic step: Applying gravity load to bring the model into geostatic equilibrium
3. Static step: Applying an axial load of 500 kN to the pile head
4. Steady-state coupled temperature-displacement step: Increasing the pile temperature and obtaining a temperature field based on the steady-state heating conditions
5. Dynamic step: Applying earthquake motion to the base of the model.

For regular pile analyses, the heating step was excluded and the remaining steps were the same. Consequently, earthquake responses of regular and energy piles were compared in terms of acceleration, lateral displacement, and vertical displacements. Pile head stiffness was used in comparison of axially loaded piles which is given in Equation 3.1 (Tehrani et al., 2016).

$$P_H = \frac{P}{D.G.w_t} \tag{3.1}$$

where P_H is the pile head stiffness, P is the axial load (kN), D is the pile diameter (m), *G* is the soil shear modulus (kPa), and w_t is the pile head displacement (m).

CHAPTER 4

RESULTS AND DISCUSSION

4.1. Discussion of Results Prior to Earthquake Excitation

Prior to earthquake analysis, vertical displacements along pile length under the effect of mechanical loading and heating were shown in Figure 4.1.

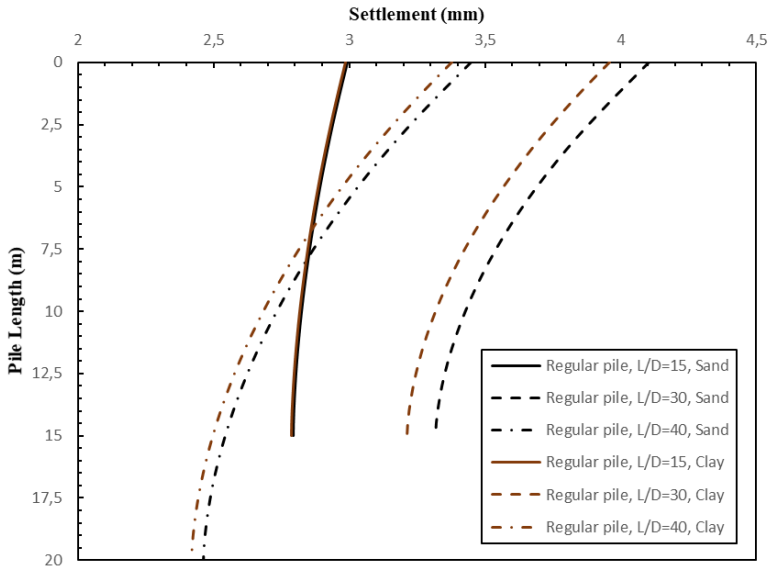

(a)

Figure 4.1. Settlement along pile length under (a) no heating, (b) ΔT=21°C, (c) ΔT=30°C

(cont. on next page)

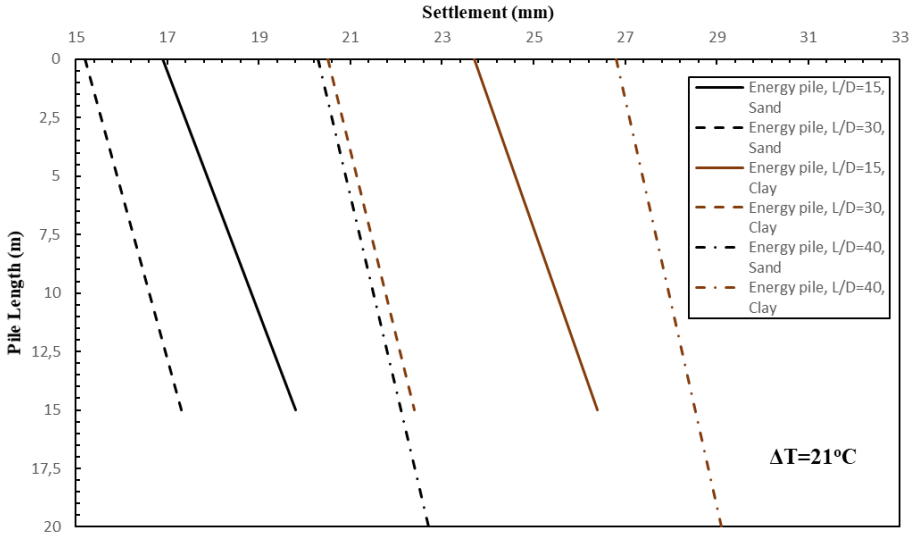

(b)

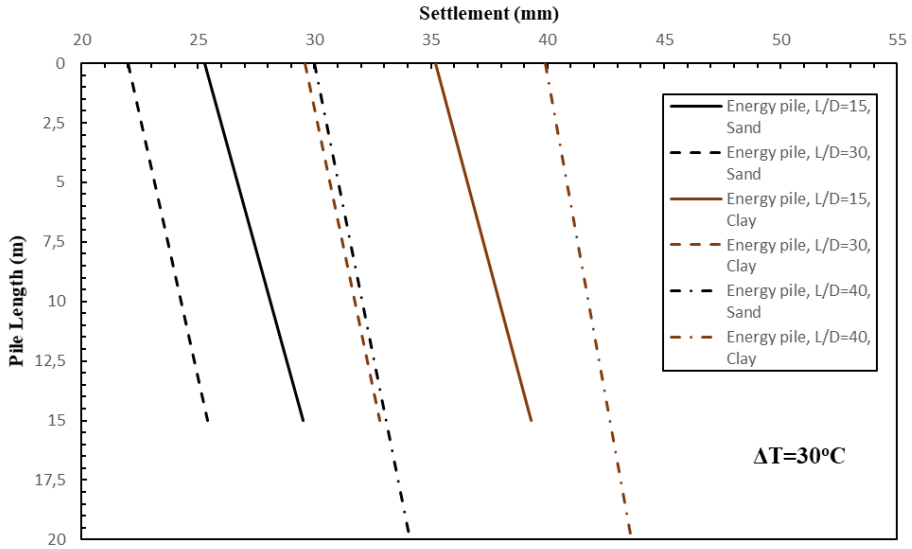

(c)

Figure 4.1 (cont.)

As seen in Figure 4.1 (a), displacements are around 3 mm to 4.1 mm under static load for regular piles. Maximum settlements were observed at the pile head, and reduced along the pile length. Figures 4.1 (b) and 4.1 (c) show that heating causes a significant increase in pile head settlements of energy piles. For example, for the pile with L/D=40, which was placed in clay, the settlements increased from 3.4 mm to 26.8 mm for 21ºC temperature increase, and 40 mm pile head settlement was observed for 30ºC temperature increase. Moreover, the maximum settlements were observed at pile toe indicating that

pile expands due to heating and pile head displacing upward, resulting in a reduction in pile head settlements. Without any temperature increase, the settlement of the pile in clay was relatively smaller than the pile in sand. However, while a temperature-dependent cohesion was defined, the settlement of the pile in clay was significantly greater than that of the pile in sand. This can be attributed to the lower thermal expansion coefficient of the surrounding clay. The thermal expansion coefficients of sand and clay were interchanged and compared to the original results under the temperature increase of 30^{o}C as shown in Figure 4.2.

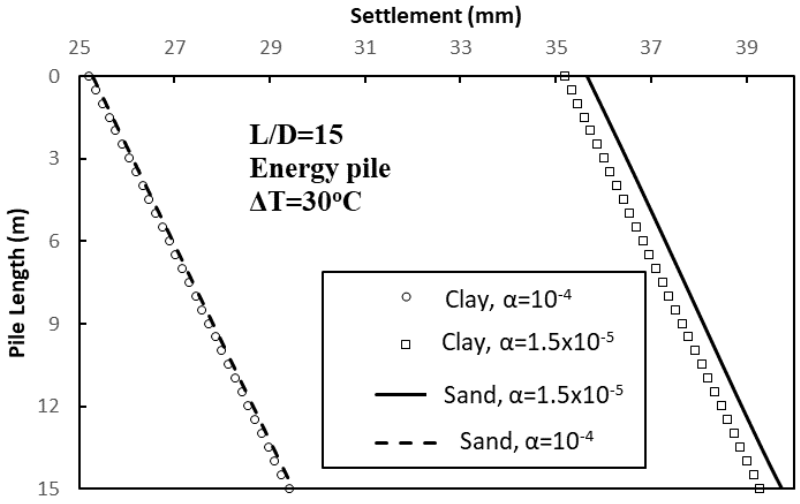

Figure 4.2. Settlements in sand and clay due to change in thermal expansion under $\Delta T=30^{o}C$

When the thermal expansion coefficient of sand and clay were interchanged, the settlement of a pile surrounded by clay was found to be reduced. The settlement of the pile placed in sand increased when the thermal expansion coefficient of clay was used. From Figure 4.2, it can also be seen that when $\alpha=1.5x10^{-5}$ for sand and clay, the settlement of clay is slightly smaller than that of sand. The parametric observation indicates that as the thermal expansion coefficient of soil is increased, surrounding soil may uplift the pile due to thermal expansion under a temperature increase. Similar behavior was observed in the work of Saggu and Chakraborty (2015).

Without heating, L/D=30 has the maximum pile head settlement, whereas L/D=15 has the minimum pile head settlement. This can be attributed to the diameter effect in axial loading, which reduces the applied stress by increasing the surface area. However, after heating, it was found that L/D=30 has the minimum pile head settlement, whereas

L/D=40 had the maximum pile head settlement. The reason for such a change is the effect of temperature distribution. It is expected that the heating effect is observed more clearly for a greater temperature field. Figures 4.3 and 4.4 show the temperature distribution in radial distance from the pile center and vertical distance from the pile at a depth of 7.5 m to demonstrate the effect of geometric properties.

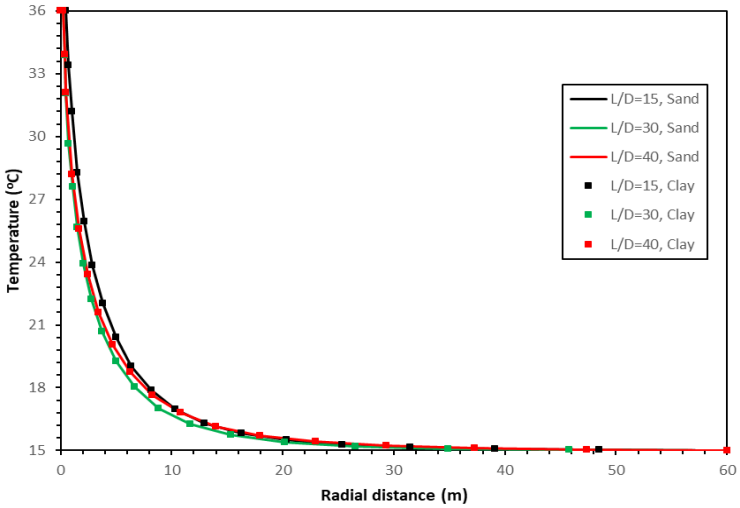

(a)

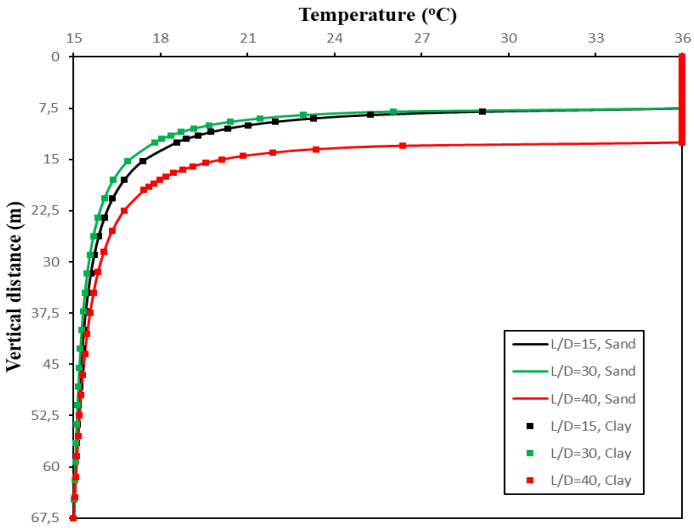

(b)

Figure 4.3. Temperature distribution under ΔT=21ºC at (a) radial distance, (b) vertical distance from the pile at a depth of 7.5 m

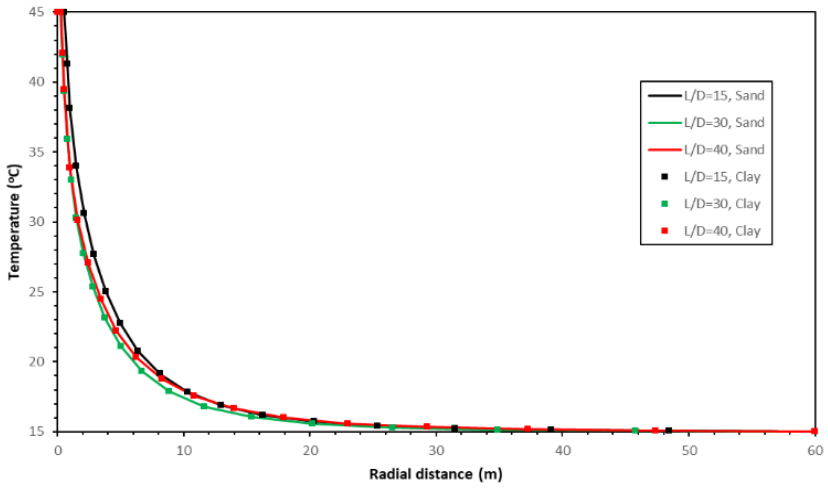

(a)

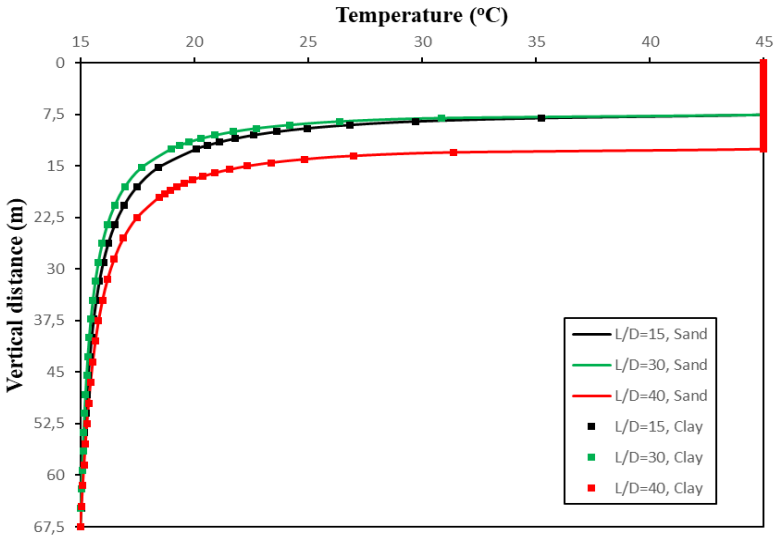

(b)

Figure 4.4. Temperature distribution under ΔT=30°C at (a) radial distance, (b) vertical distance from the pile at a depth of 7.5 m

From Figures 4.3 and 4.4, it can be seen that the radial temperature profiles of sand and clay are almost identical. Figure 4.3 (a) and 4.4 (a) show a slightly higher temperature profile for L/D=15 at a radial distance from the pile center, and temperature profiles of L/D=15, 30, and 40 are identical when the distance of nearly 18 m is reached. A higher temperature profile for L/D=40 at a vertical distance from the pile at a depth of 7.5 m can be clearly seen in Figure 4.3 (b) and 4.4 (b). The length of the pile affected the temperature distribution on the domain.

Figure 4.5 shows the vertical displacement distribution at a radial distance from the center of the pile head.

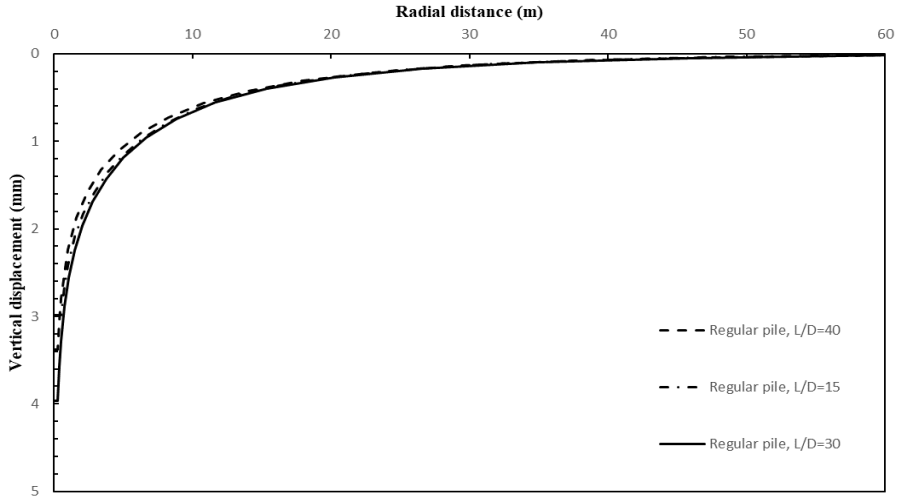

Figure 4.5. Vertical displacements on the ground surface for regular piles placed in clay

Figure 4.5 demonstrates that the vertical displacements at the boundary of the model were zero for the regular piles placed in clay. This indicates that the size of the model is appropriate for the following heating and earthquake analyses.

Table 4.1 shows the ratio of final soil elastic modulus to its initial soil elastic modulus under a temperature increase.

Table 4.1. Ratio of final soil elastic modulus to its initial soil elastic modulus under a temperature increase

ΔT (°C)	$E_{s,0}$ (MPa)	$\frac{E_{s,T}}{E_{s,0}}$
21	15	0.454
	20	0.591
	30	0.727
30	15	0.22
	20	0.415
	30	0.61

As the initial soil elastic modulus increases, the ratio of the final soil elastic modulus to initial soil elastic modulus reduces. For example, when the initial soil elastic modulus increased from 15 to 30 MPa, the ratio became approximately three times greater

under a temperature increase of 30 ºC, which corresponds to 61% of the initial soil elastic modulus. An increase in the initial soil elastic modulus may decrease the significance of displacements induced by heating. In order to prove this statement, a pile with L/D=30 was placed in sand, in which the initial soil elastic modulus was increased to 30 MPa and subjected to 500 kN axial load. The response of pile under no heating, heating to 21ºC, and heating to 30ºC is compared. The comparison of results are demonstrated in Figure 4.6.

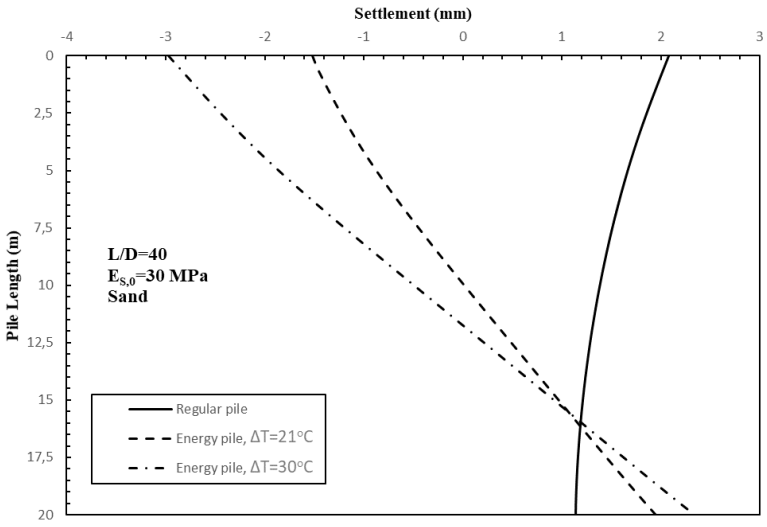

Figure 4.6. Settlements on the pile body placed in sand with $E_{S,0}$=30 MPa

Figure 4.6 shows that the energy piles were elongated from both ends in opposite directions due to the thermal expansion. The pile head settlement of the regular pile was 2 mm, and the pile toe of the regular pile displaced 1 mm. However, the pile head of the energy pile with a temperature increase of 21ºC displaced 1.5 mm in upward direction, and the pile toe displaced 2 mm in downward direction. Similarly, the pile head of the energy pile with a temperature increase of 30ºC displaced 3 mm in upward direction, and the pile toe displaced 2.2 mm in downward direction. Moreover, the displacements at around 16 m depth were the same for the regular pile and the energy piles, which may indicate the existence of the null-point. Null-point means there is no thermally induced vertical displacements, around that depth (Bourne-Webb et al., 2009; Khosravi et al., 2016). Similar observations were made in the work of Khosravi et al. (2016). The findings indicate that the energy piles elongate from both ends in opposite directions due to the thermal expansion, and the direction of elongation depends on the location of the null-point. In addition, the effect of the temperature-dependent soil elastic modulus on the behavior of the energy piles placed in the soil with 30 MPa initial soil elastic modulus

was negligible, and the displacement behavior of the energy piles was mainly governed by the thermal expansion coefficient.

The following earthquake response studies were carried out using soils with 15 MPa initial soil elastic modulus.

4.2. Earthquake Responses of Energy Piles and Identical Regular Piles

Earthquake response of a vertically loaded energy pile for L/D ratios of 15, 30, and 40 were evaluated in terms of acceleration, lateral displacement, and vertical displacement. The responses of a regular pile, an energy pile heated to 36°C, shown as T=36, and an energy pile heated to 45°C, shown as T=45, were compared. The measurements were taken from the node at the center of the pile head.

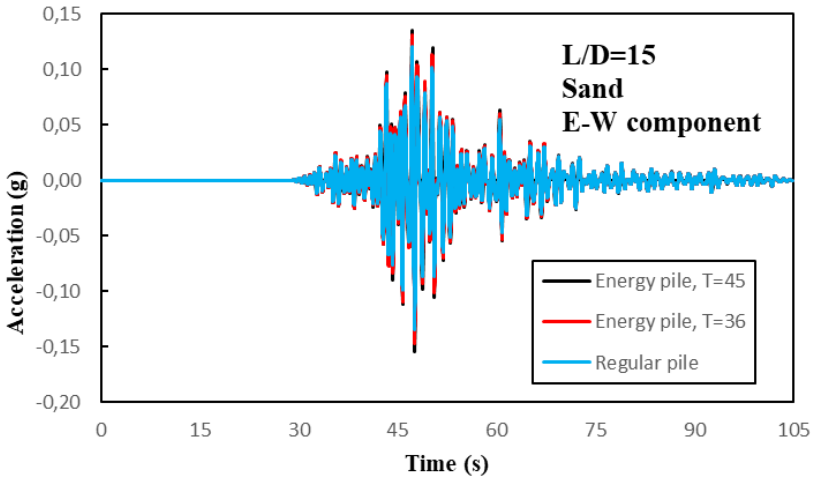

(a)

Figure 4.7. (a) Acceleration response, (b) Lateral displacement, (c) Vertical displacement of pile with L/D=15 placed in sand subjected to input motion of E-W component of 2020 Izmir Earthquake

(cont. on next page)

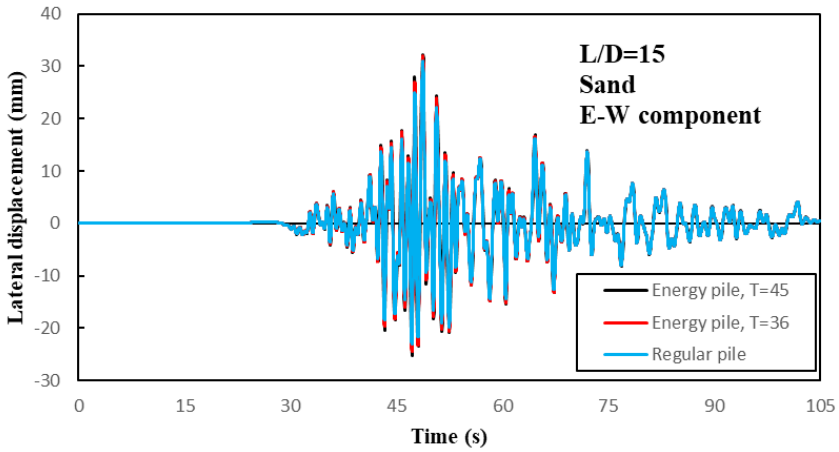

(b)

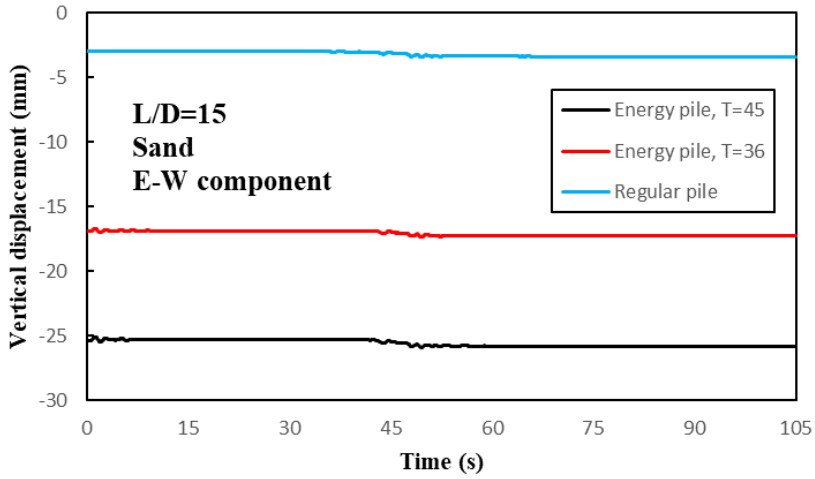

(c)

Figure 4.7 (cont.)

The pile with an L/D ratio of 15 placed in sand under the E-W component of the motion was investigated under no heating, heating to 36, and heating to 45ºC. Peak accelerations were 0.135, 0.147, and 0.154g, respectively. The peak lateral displacements of the regular pile, and the energy piles heated to 36 and heated to 45ºC were nearly 30.9, 31.95 and 32.3 mm, respectively. Nearly 0.02g and 1.5 mm increase in acceleration and lateral displacement of piles under heating were considered as a slight increase. Peak pile head settlement induced by earthquake excitation was 3.4, 17.3, and 25.9 mm for the regular pile and the energy piles, which shows nearly a 22.5 mm maximum increase in settlement due to heating.

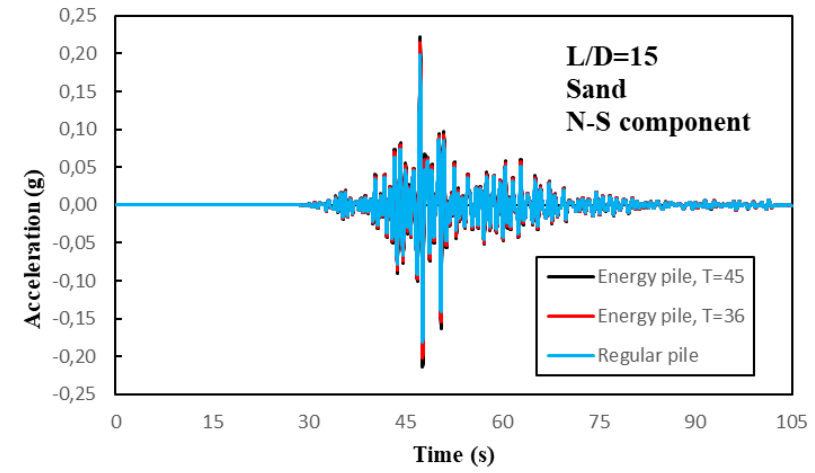

(a)

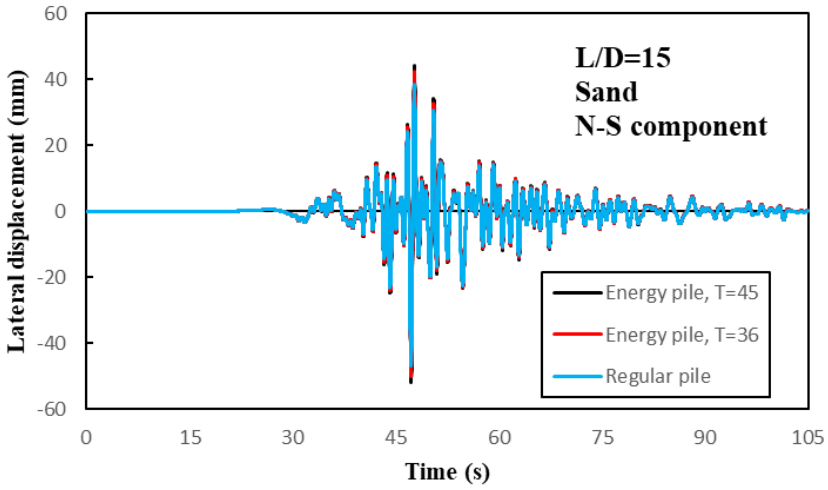

(b)

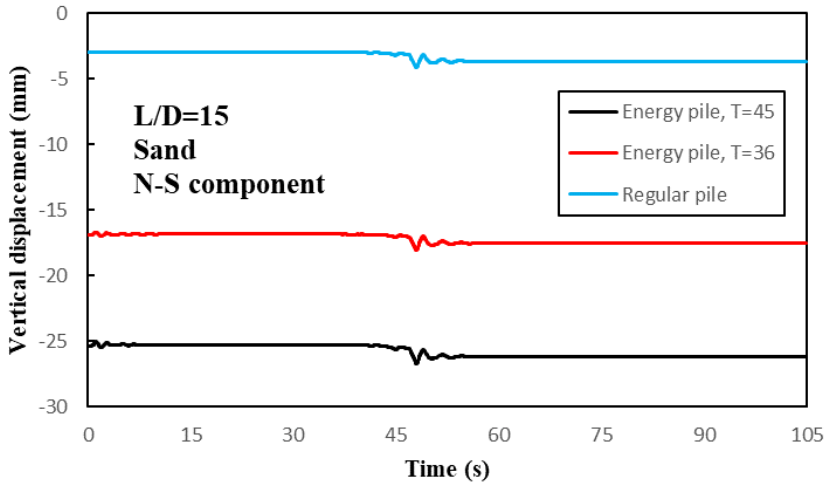

(c)

Figure 4.8. (a) Acceleration response, (b) Lateral displacement, (c) Vertical displacement of pile with L/D=15 placed in sand subjected to input motion of N-S component of 2020 Izmir Earthquake

Figure 4.8 demonstrates that the temperature increase of 30ºC caused a considerable increase in acceleration and lateral displacement response. Moreover, the effect of heating on the vertical displacement of the axially loaded energy pile was found to be significant. The peak acceleration and lateral displacements were 0.2g and 47.1 mm for the regular pile, 0.22g and 51.9 mm for the energy pile heated to 45ºC, which corresponds to a 12% increase in acceleration and a 10% increase in lateral displacement due to heating. Peak vertical displacement of the regular pile and energy pile heated to 45ºC were 4.1 mm and 26.75 mm, respectively. It indicates that the settlement of the energy pile was at least 5.5 times greater than that of the regular pile.

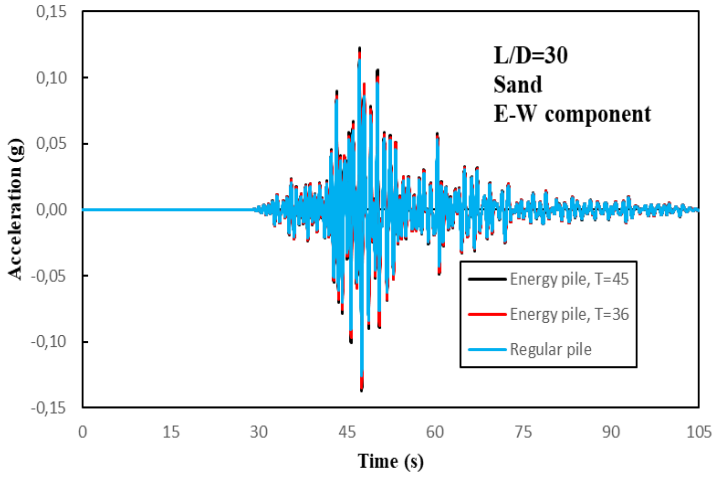

(a)

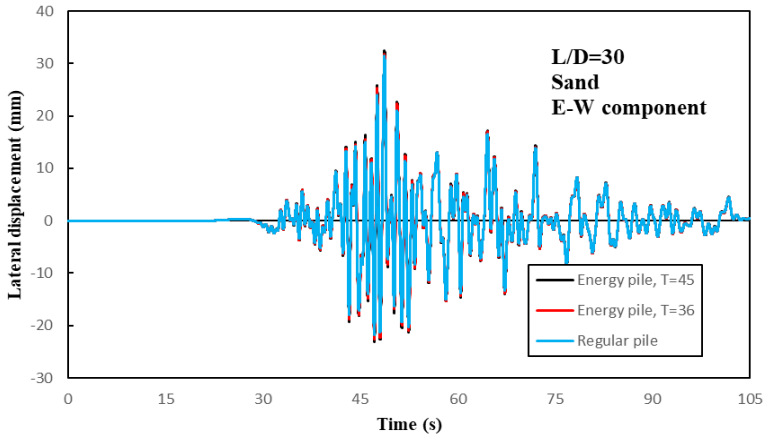

(b)

Figure 4.9. (a) Acceleration response, (b) Lateral displacement, (c) Vertical displacement of pile with L/D=30 placed in sand subjected to input motion of E-W component of 2020 Izmir Earthquake

(cont. on next page)

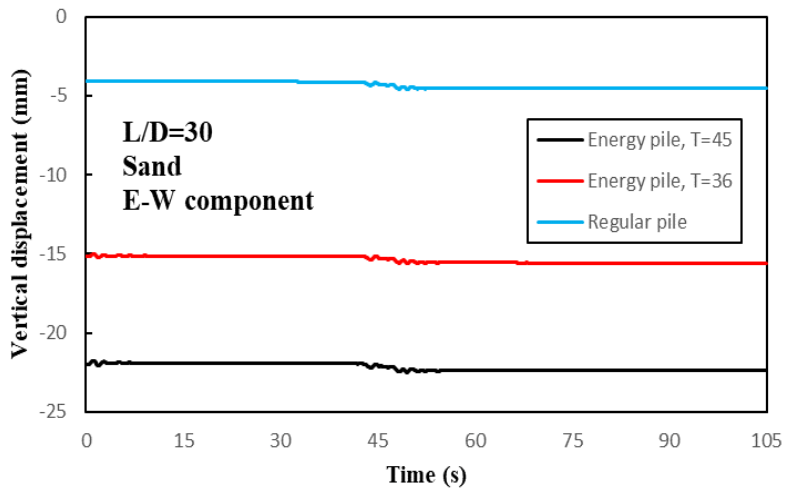

(c)

Figure 4.9 (cont.)

Peak accelerations of the regular pile, energy pile heated to 36ºC and 45ºC were 0.13g, 0.135g and 0.14g, respectively. Peak lateral displacement of regular pile and energy pile heated to 36ºC and 45ºC were 31.4 mm, 31.8 mm and 32.5 mm, respectively. 1.1 mm increase in peak lateral displacement of the pile under the temperature increase of 30ºC is negligible. The peak pile head settlements were 4.6 mm, 15 mm and 22.5 mm for the regular pile and the energy piles heated to 36ºC and 45ºC, respectively.

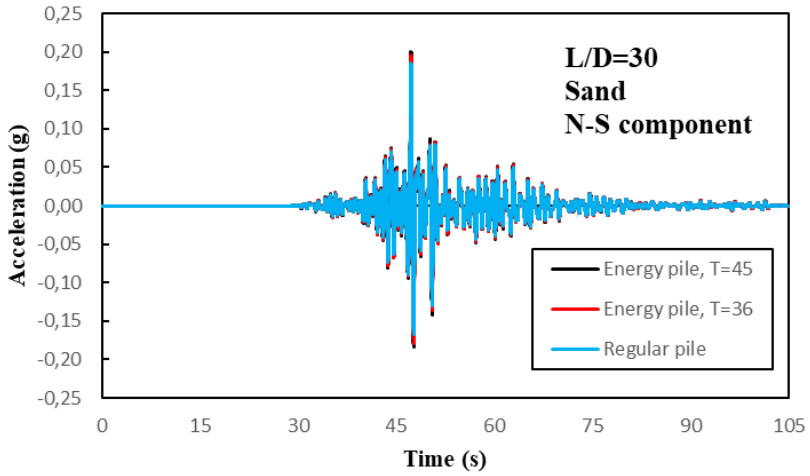

(a)

Figure 4.10. (a) Acceleration response, (b) Lateral displacement, (c) Vertical displacement of pile with L/D=30 placed in sand subjected to input motion of N-S component of 2020 Izmir Earthquake

(cont. on next page)

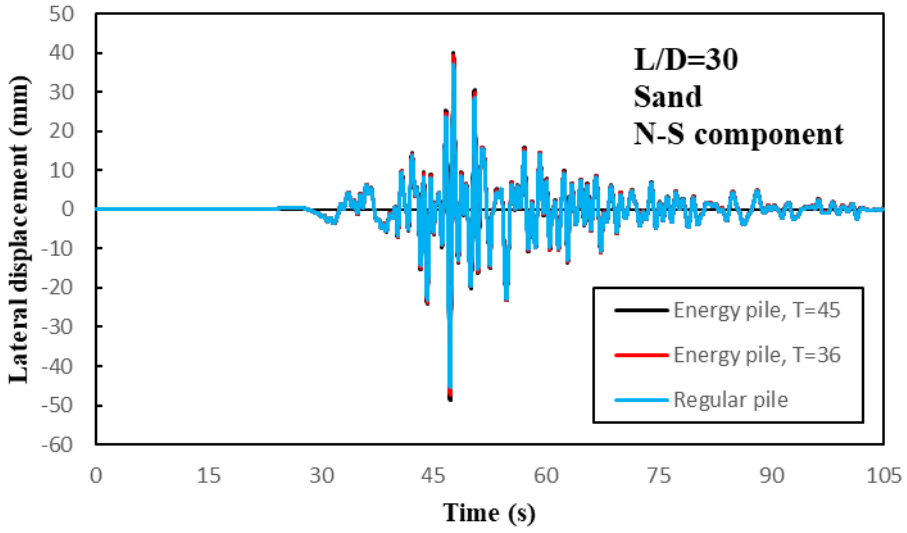

(b)

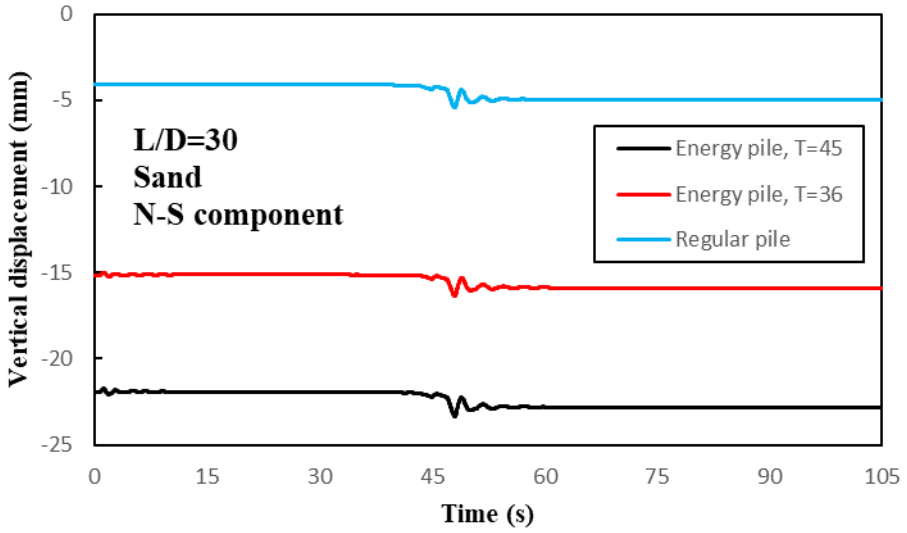

(c)

Figure 4.10 (cont.)

Similar observations were made for the pile having an L/D ratio of 30 under the N-S component of the input motion. Peak acceleration of regular pile, energy piles heated to 36 and 45^{o}C were, respectively, 0.186g, 0.195g, and 0.2g, which indicates a very slight increase. Peak lateral displacement of regular pile and energy pile heated to 45^{o}C were, respectively, 45.5, 47.4 and 48.6 mm. Peak lateral displacement of the energy pile indicates a slight increase of 7% due to heating. The peak head settlement of the energy pile was 23.4 mm, which is 330% greater than the peak head settlement of a regular pile.

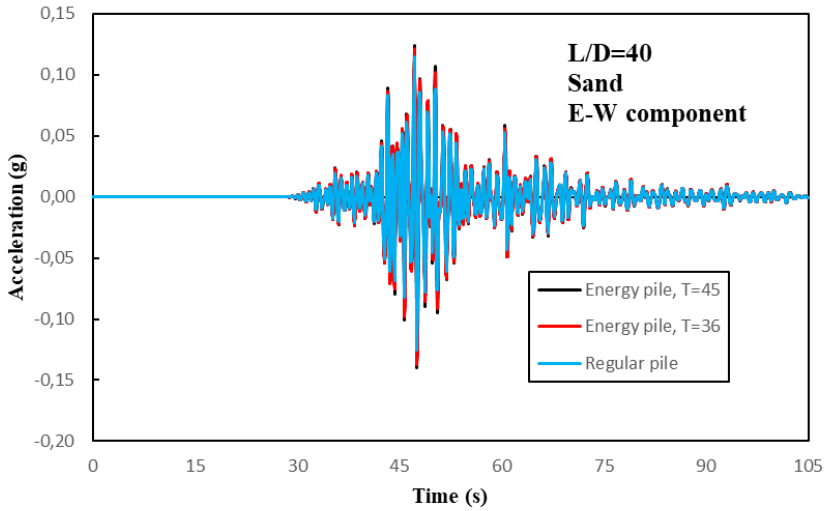

(a)

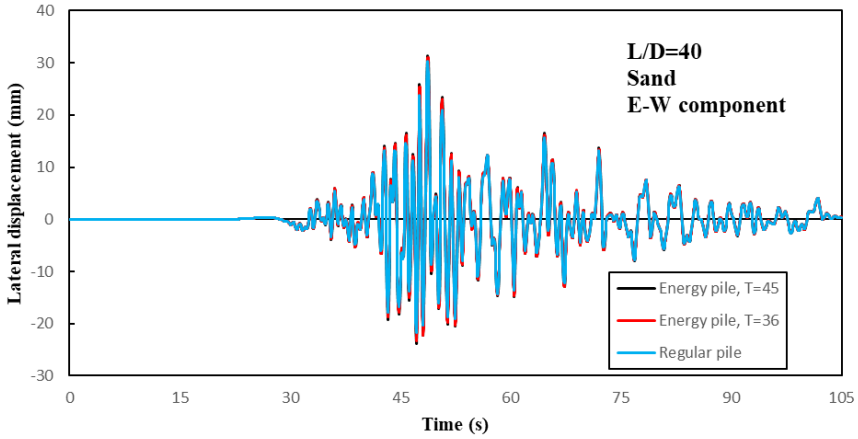

(b)

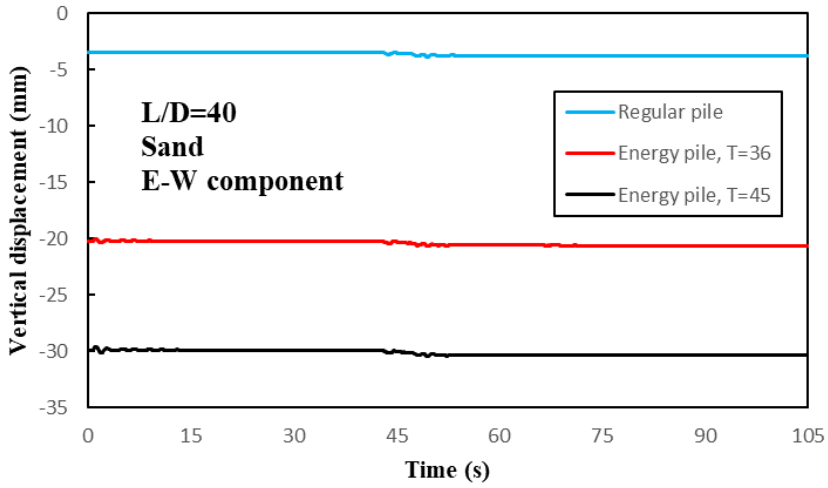

(c)

Figure 4.11. (a) Acceleration response, (b) Lateral displacement, (c) Vertical displacement of pile with L/D=40 placed in sand subjected to input motion of E-W component of 2020 Izmir Earthquake

The peak acceleration of the regular pile and energy pile heated to 45°C for L/D=40 placed in the sand were 0.13g and 0.14g, respectively. Similar to the response of L/D=30 under E-W component of the earthquake motion, 1 mm increase in lateral displacement of the energy pile due to heating was observed, which is nearly the same as with the regular pile. Peak pile head settlements were 3.9 mm, 20.6 mm and 30.5 mm for the regular pile, and the energy piles heated to 36 and 45°C, respectively.

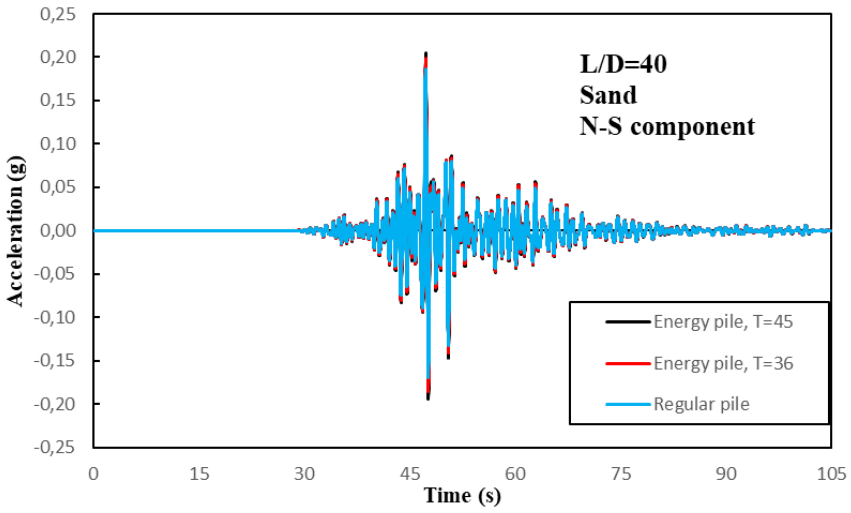

(a)

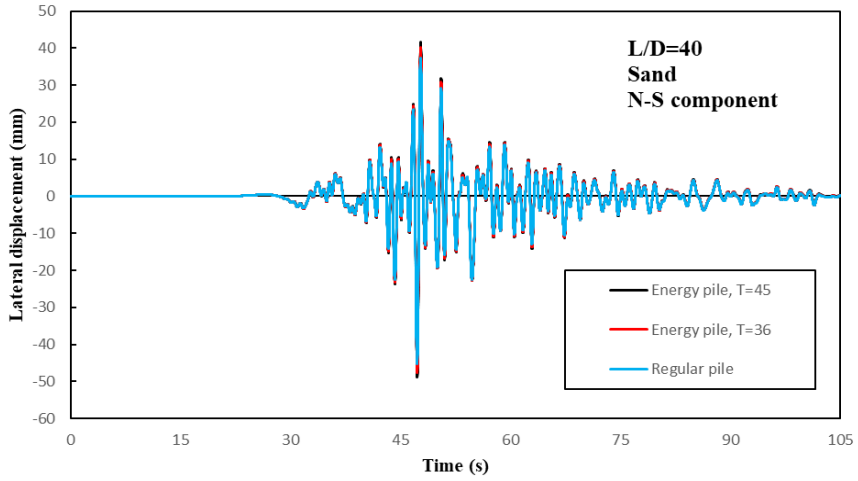

(b)

Figure 4.12. (a) Acceleration response, (b) Lateral displacement, (c) Vertical displacement of pile with L/D=40 placed in sand subjected to input motion of N-S component of 2020 Izmir Earthquake

(cont. on next page)

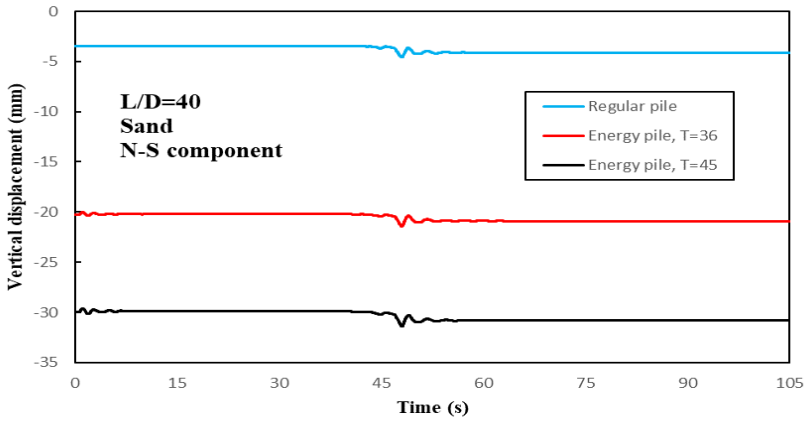

(c)

Figure 4.12 (cont.)

The pile with an L/D ratio of 40 placed in sand under the N-S component of the motion was investigated under no heating, heating to 36, and heating to 45ºC. Peak accelerations were 0.187, 0.199, and 0.205g, respectively. The peak lateral displacements of the regular pile, and the energy piles heated to 36 and heated to 45ºC were nearly 45.3, 47.7 and 48.9 mm, respectively. Nearly 0.02g and 3.6 mm increase in acceleration and lateral displacement of piles under heating were considered as a slight increase. Peak pile head settlement induced by earthquake excitation was 4.6, 21.4, and 31.4 mm for the regular pile and the energy piles, which shows nearly a 27 mm maximum increase in settlement due to heating.

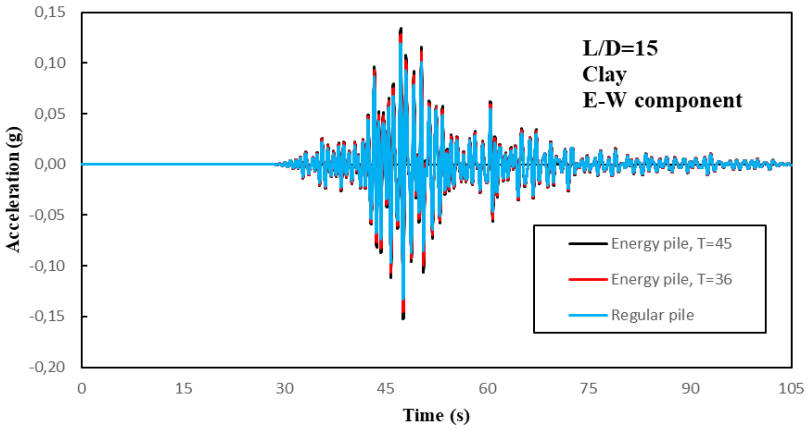

(a)

Figure 4.13. (a) Acceleration response, (b) Lateral displacement, (c) Vertical displacement of pile with L/D=15 placed in clay subjected to input motion of E-W component of 2020 Izmir Earthquake

(cont. on next page)

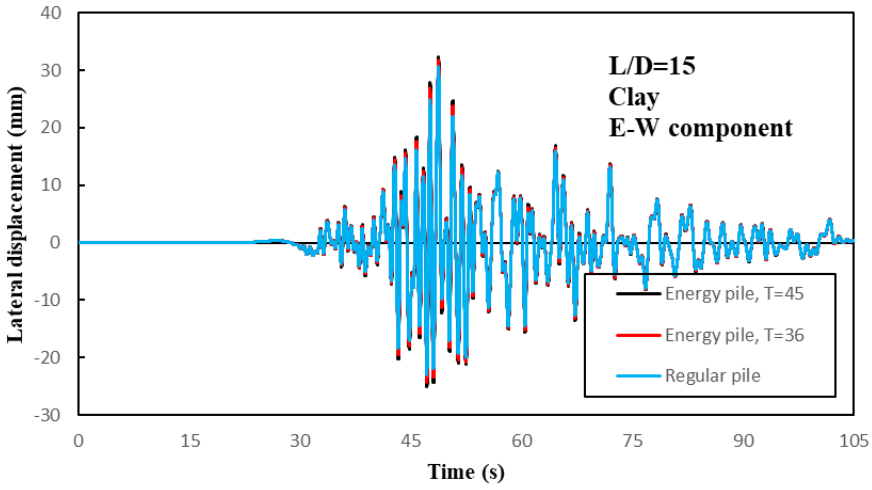

(b)

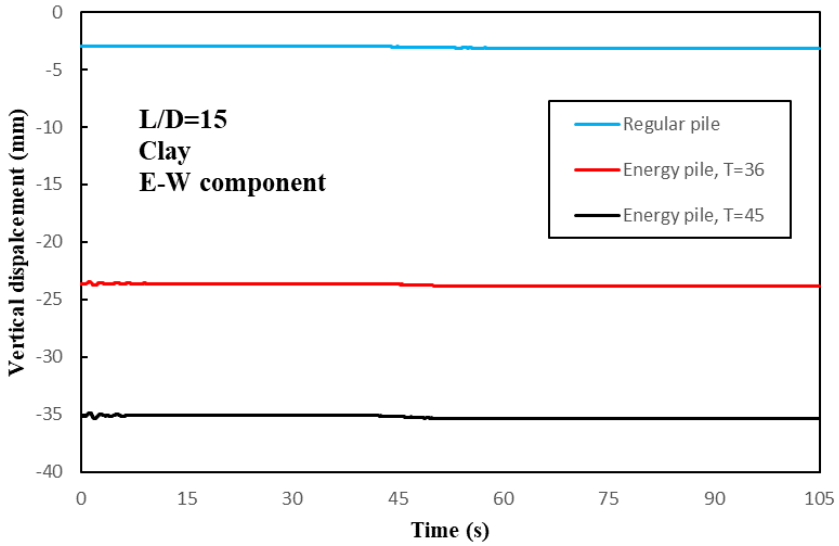

(c)

Figure 4.13 (cont.)

The responses of piles with L/D=15 placed in clay under the E-W component of earthquake motion are demonstrated in Figure 4.13. As the temperature of the pile increased, a slight increase in acceleration and lateral displacements increased, according to Figures 4.13 (a) and 4.13 (b). The increase in vertical displacements was significant. The displacement of the pile increased from 3.2 mm to 23.9 mm when the pile was heated to 36^{o}C. When the pile was heated to 45^{o}C, the displacement of the pile increased from 3.2 mm to 35.5 mm.

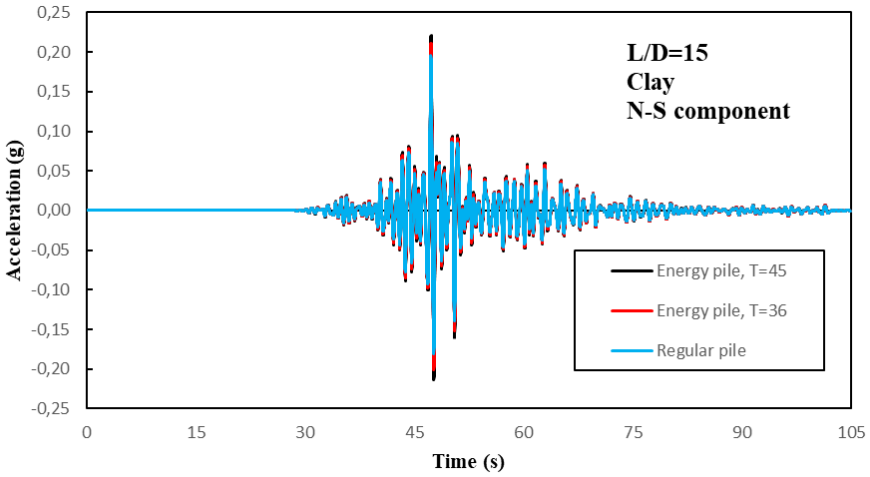

(a)

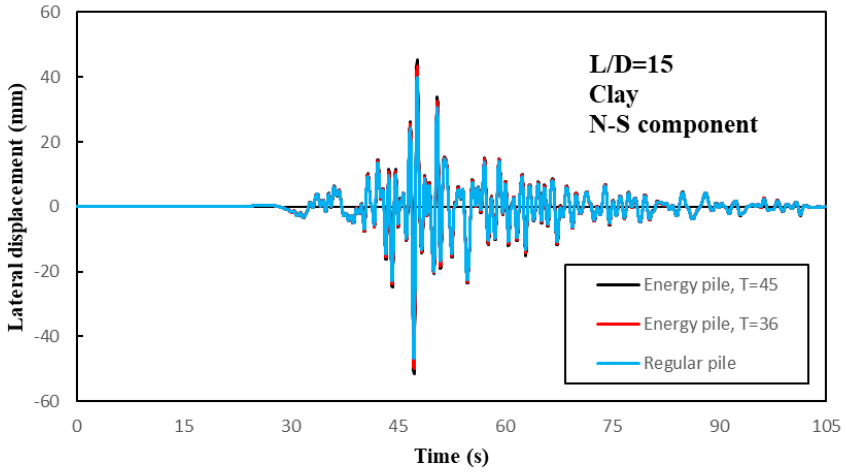

(b)

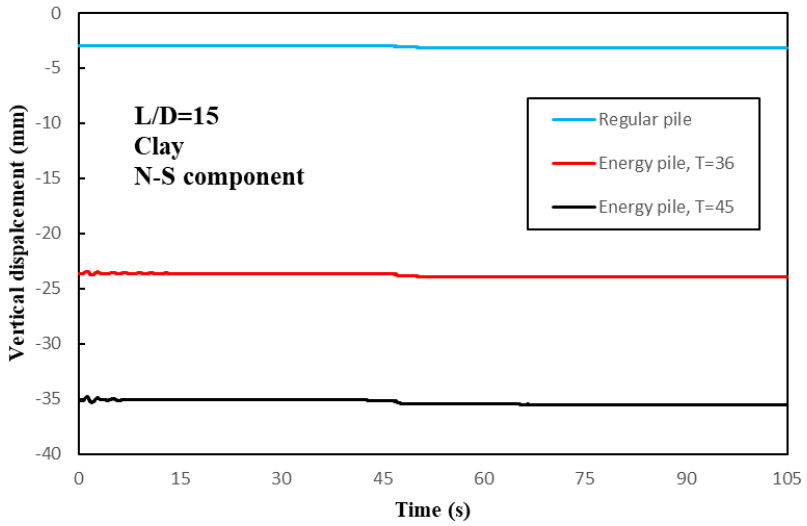

(c)

Figure 4.14. (a) Acceleration response, (b) Lateral displacement, (c) Vertical displacement of pile with L/D=15 placed in clay subjected to input motion of N-S component of 2020 Izmir Earthquake

The pile with an L/D ratio of 15 under the N-S component of the input motion exhibits greater acceleration and lateral displacement responses than the E-W component. Peak acceleration was 0.195g for the regular pile under the N-S component, whereas the peak acceleration was 0.133g for the regular pile under the E-W component of the motion. Peak lateral displacement of the regular pile was 46.8 mm, which was 16 mm greater than the peak lateral displacement of the regular pile under E-W component of the motion. When the pile was heated to 45ºC, nearly 5 mm increase in peak lateral displacement was observed under the N-S component of the motion, whereas 1.5 mm increase was observed under the E-W component. However, the increase in vertical displacements was significant under the E-W and N-S components of the input motion. The pile exhibited 20.7 mm increase in vertical displacements when the pile was heated to 36ºC. When the pile was heated to 45ºC, the displacement of the pile was nearly 32.5 mm increased.

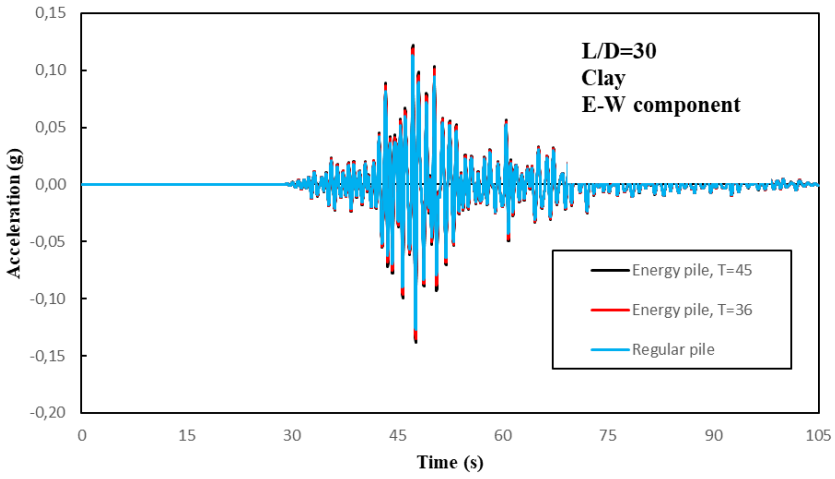

(a)

Figure 4.15. (a) Acceleration response, (b) Lateral displacement, (c) Vertical displacement of pile with L/D=30 placed in clay subjected to input motion of E-W component of 2020 Izmir Earthquake

(cont. on next page)

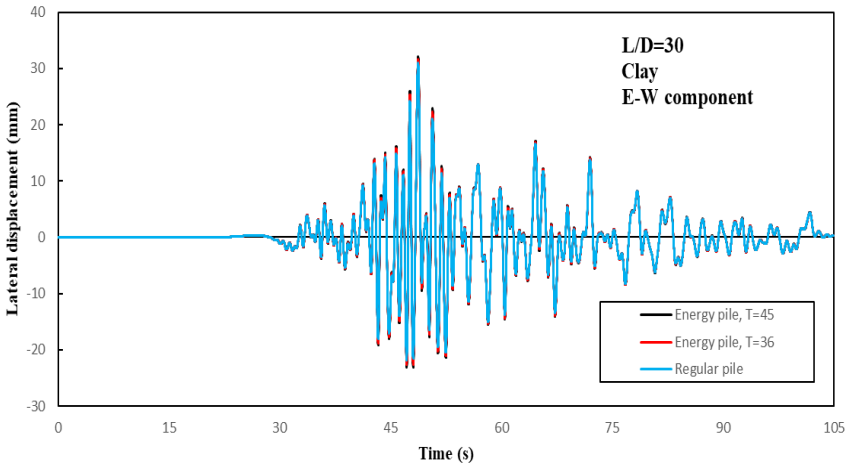

(b)

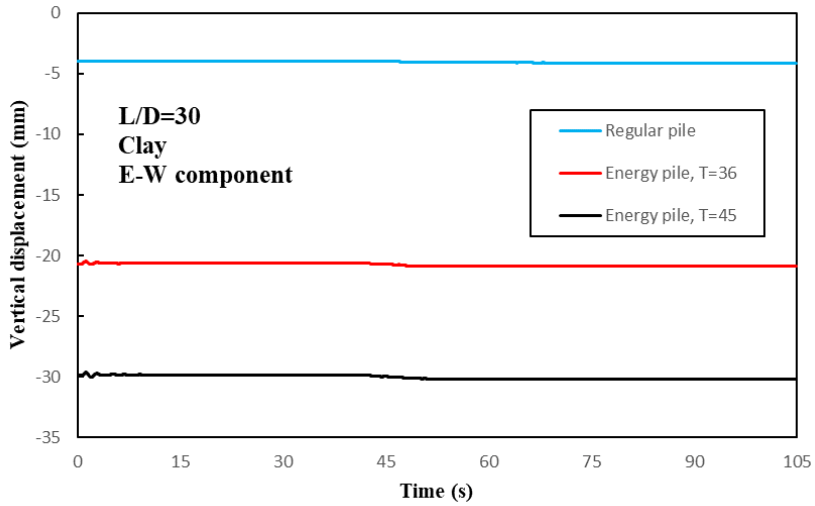

(c)

Figure 4.15 (cont.)

Response of piles having L/D=30 placed in clay shows a similar behavior where acceleration and lateral displacements slightly increased, as shown in Figures 4.15 (a) and 4.15 (b). However, the vertical displacement due to heating reach 21.4 mm for heating the pile to 36^{o}C and 30.4 mm for heating the pile to 45^{o}C.

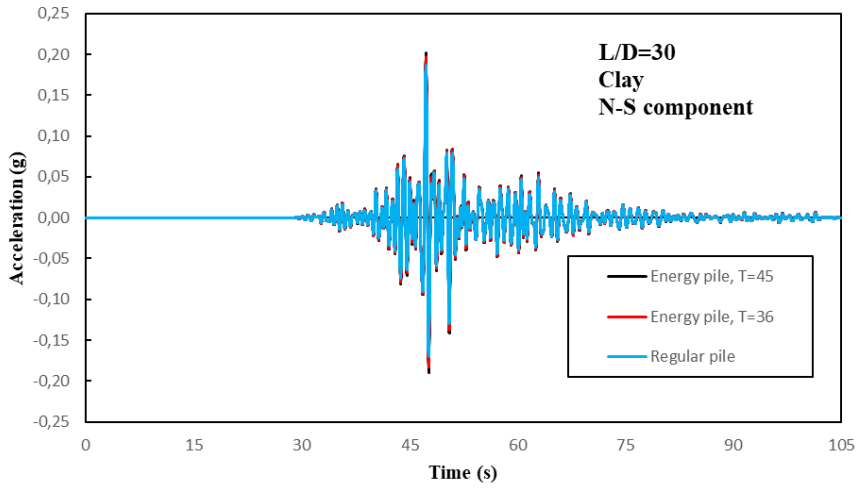

(a)

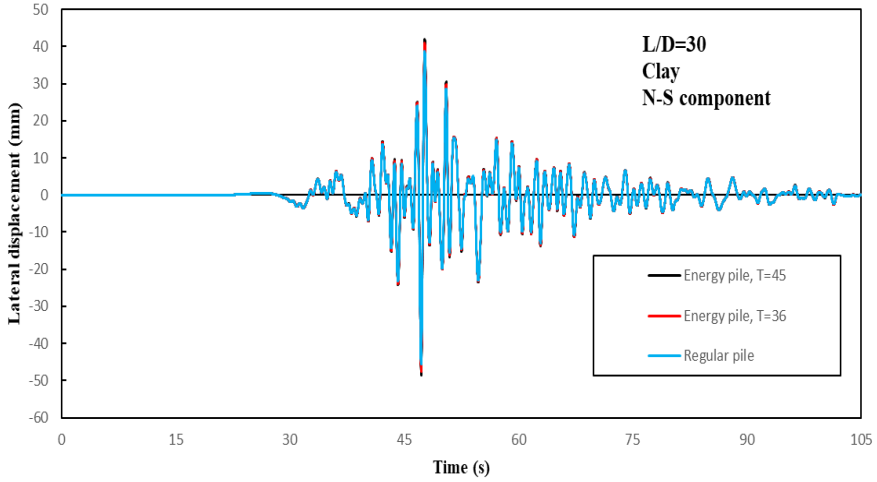

(b)

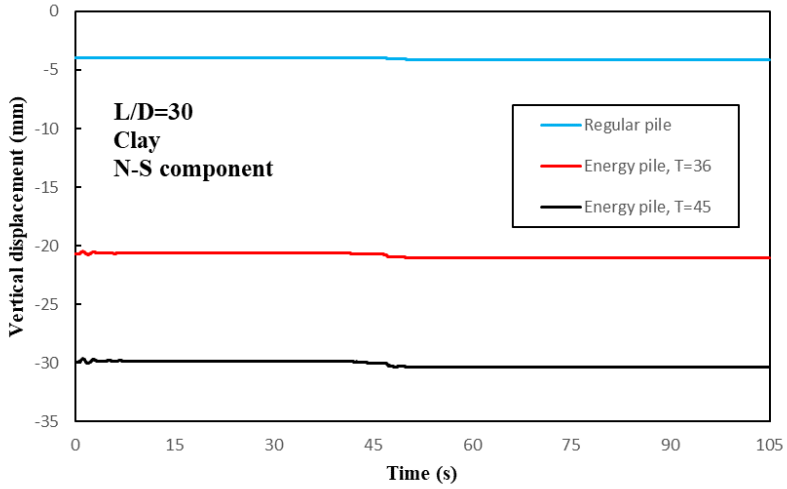

(c)

Figure 4.16. (a) Acceleration response, (b) Lateral displacement, (c) Vertical displacement of pile with L/D=30 placed in clay subjected to input motion of N-S component of 2020 Izmir Earthquake

Similarly, slight increases in peak acceleration and lateral displacements were observed for the pile with L/D=30 placed in clay subjected to the N-S component of the earthquake motion. Vertical displacements of the pile was increased 17 mm when the pile was heated to 36^{o}C, and 27.2 mm increase was observed when the pile was heated to 45^{o}C.

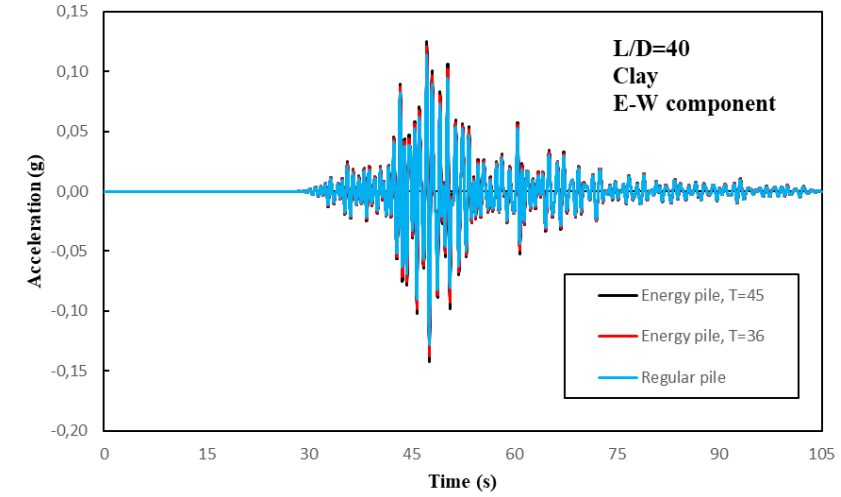

(a)

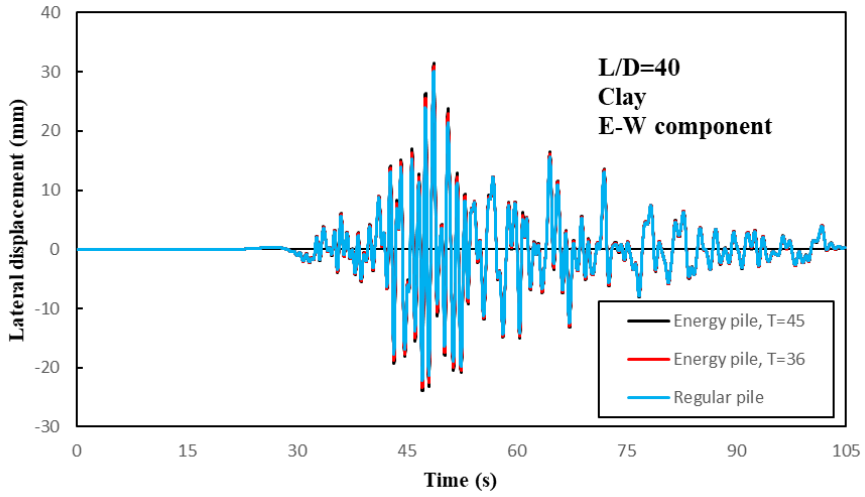

(b)

Figure 4.17. (a) Acceleration response, (b) Lateral displacement, (c) Vertical displacement of pile with L/D=40 placed in clay subjected to input motion of E-W component of 2020 Izmir Earthquake

(cont. on next page)

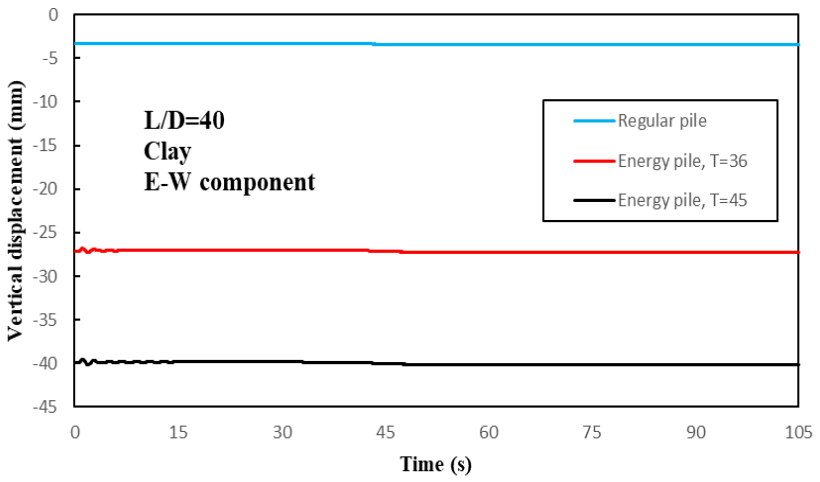

(c)

Figure 4.17 (cont.)

Similarly, slight increases in peak acceleration and lateral displacements were observed for the pile with L/D=40 placed in clay subjected to E-W component of the 2020 Izmir Earthquake. However, the increase in peak vertical displacements due to heating was found to be substantial.

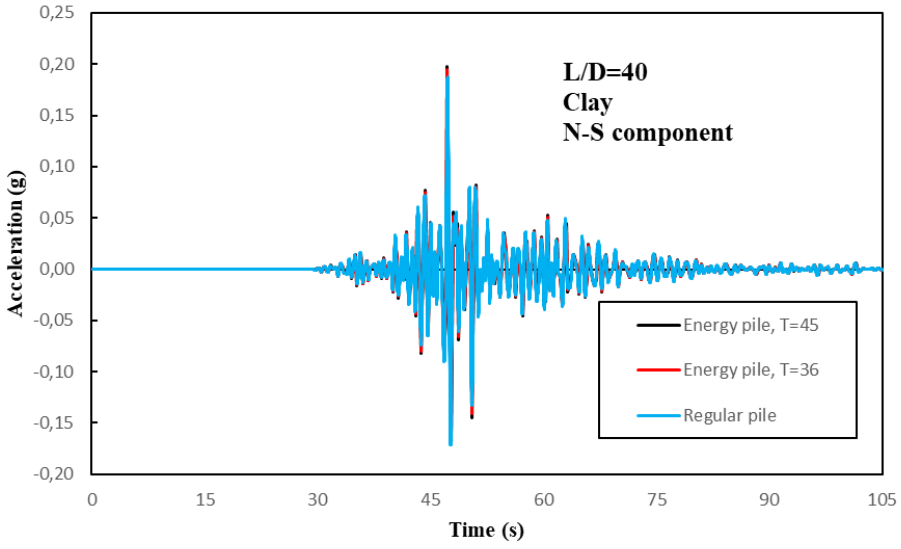

(a)

Figure 4.18. (a) Acceleration response, (b) Lateral displacement, (c) Vertical displacement of pile with L/D=40 placed in clay subjected to input motion of N-S component of 2020 Izmir Earthquake

(cont. on next page)

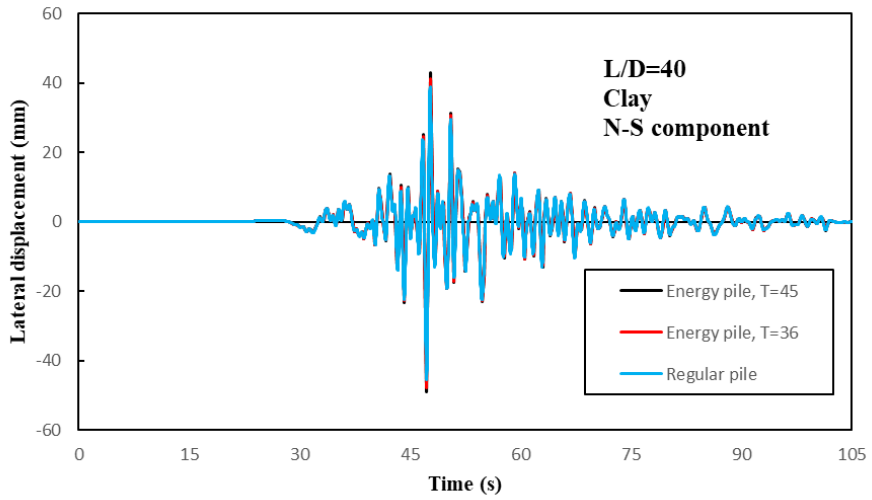

(b)

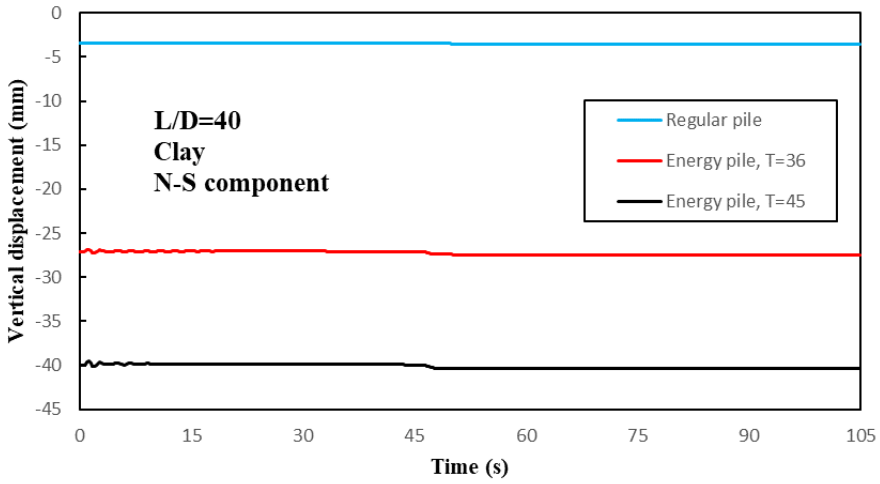

(c)

Figure 4.18 (cont.)

From Figures 4.7 to 4.18, a pattern was captured in which acceleration and lateral displacement responses of energy piles exhibited a slight increase as the temperature increased under the 2020 Izmir earthquake motion, and a significant increase in vertical displacements were observed due to heating. For L/D=40, heating the pile to 45 ^{o}C caused a settlement of around 40.4 mm settlements on the pile head. The expectation for sand was fulfilled as the reduced soil stiffness caused a greater settlement response under the earthquake excitation. However, the shear strength of clay was increased upon heating and observations were not clear on the effect of temperature dependency of cohesion. Moreover, the larger settlements on piles placed in clay were attributed to the smaller thermal expansion coefficient, so the uplift of the pile due to soil expansion had become smaller and caused larger settlements. Therefore, unlike the findings of Cekerevac and

Laloui (2010), heating did not increase the earthquake resistance of the clay, and the effect of the temperature-dependent soil elastic modulus on the earthquake response of the clay was found to be more substantial.

Absolute values of the peak responses are tabulated in Table 4.2 to summarize the findings of the earthquake response of energy piles.

Table 4.2. Peak responses of the piles under earthquake excitation

Model ID	Peak acceleration (g)	Peak lateral displacement (mm)	Peak vertical displacement (mm)
L/D=15, Sand, E-W	0.135	30.905	3.437
L/D=15, Sand, T=36, E-W	0.147	31.945	17.349
L/D=15, Sand, T=45, E-W	0.154	32.282	25.894
L/D=15, Sand, N-S	0.199	47.086	4.144
L/D=15, Sand, T=36, N-S	0.214	50.174	18.071
L/D=15, Sand, T=45, N-S	0.223	51.911	26.753
L/D=30, Sand, E-W	0.126	31.420	4.604
L/D=30, Sand, T=36, E-W	0.135	31.810	15.620
L/D=30, Sand, T=45, E-W	0.137	32.535	22.498
L/D=30, Sand, N-S	0.186	45.535	5.436
L/D=30, Sand, T=36, N-S	0.196	47.423	16.392
L/D=30, Sand, T=45, N-S	0.201	48.615	23.368
L/D=40, Sand, E-W	0.126	30.368	3.858
L/D=40, Sand, T=36, E-W	0.137	31.061	20.682
L/D=40, Sand, T=45, E-W	0.140	31.313	30.454
L/D=40, Sand, N-S	0.187	45.299	4.589
L/D=40, Sand, T=36, N-S	0.199	47.732	21.428
L/D=40, Sand, T=45, N-S	0.205	48.882	31.396
L/D=15, Clay, E-W	0.133	30.708	3.127
L/D=15, Clay, T=36, E-W	0.145	31.764	23.836
L/D=15, Clay, T=45, E-W	0.152	32.385	35.371
L/D=15, Clay, N-S	0.195	46.794	3.163
L/D=15, Clay, T=36, N-S	0.211	49.920	23.943
L/D=15, Clay, T=45, N-S	0.221	51.537	35.518
L/D=30, Clay, E-W	0.127	31.014	4.103
L/D=30, Clay, T=36, E-W	0.135	31.690	20.905
L/D=30, Clay, T=45, E-W	0.138	32.073	30.193
L/D=30, Clay, N-S	0.187	45.610	4.144
L/D=30, Clay, T=36, N-S	0.197	47.572	21.057
L/D=30, Clay, T=45, N-S	0.202	48.523	30.390
L/D=40, Clay, E-W	0.128	30.084	3.514
L/D=40, Clay, T=36, E-W	0.137	30.937	27.323
L/D=40, Clay, T=45, E-W	0.142	31.387	40.195
L/D=40, Clay, N-S	0.188	45.395	3.548
L/D=40, Clay, T=36, N-S	0.195	47.932	27.469
L/D=40, Clay, T=45, N-S	0.198	49.106	40.399

The peak accelerations of N-S and E-W components of the 2020 Izmir earthquake were 0.153g and 0.112g, respectively. In Table 4.2, the peak accelerations on the pile head indicate that the soil amplified the earthquake response. For example, the peak acceleration observed on the pile head with L/D=15 placed in sand under the N-S

component of the 2020 Izmir earthquake was 0.199g, which is greater than the peak input acceleration of N-S component of the 2020 Izmir earthquake. The maximum increase in lateral response due to heating was observed for piles having L/D=15, which undergone almost a 5 mm increase in lateral displacements. The response of the pile having L/D=30 placed in sand under the E-W component of the earthquake motion showed a negligible increase in lateral displacement, which is 1.1 mm due to heating. The N-S component of the earthquake motion exhibited a slight increase in lateral response due to heating, which is 3.1 mm, larger than that of the E-W component. The difference in peak lateral displacement for energy piles and regular piles may depend on the ground motion.

Based on the data in Table 4.2, the L/D ratio versus pile head stiffness under different temperature variations was plotted as given in Figures 4.19, 4.20, 4.21 and 4.22.

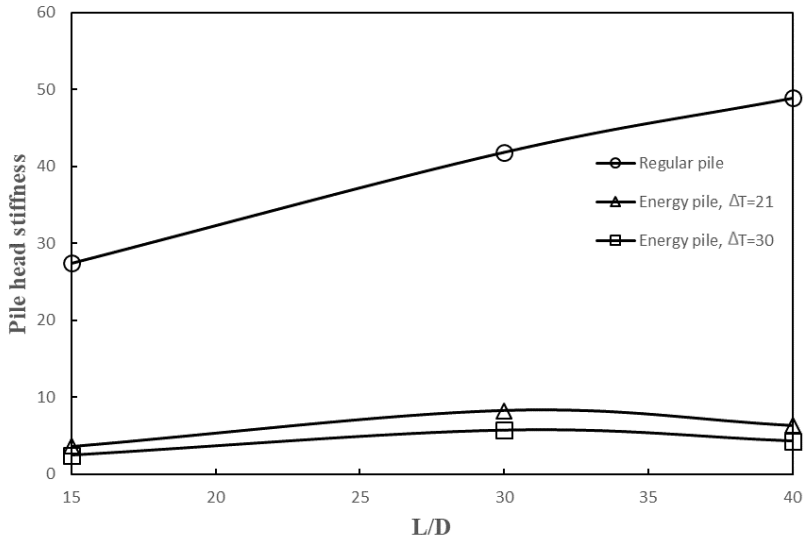

Figure 4.19. L/D versus pile head stiffness under the N-S component of the 2020 Izmir earthquake for the piles placed in clay

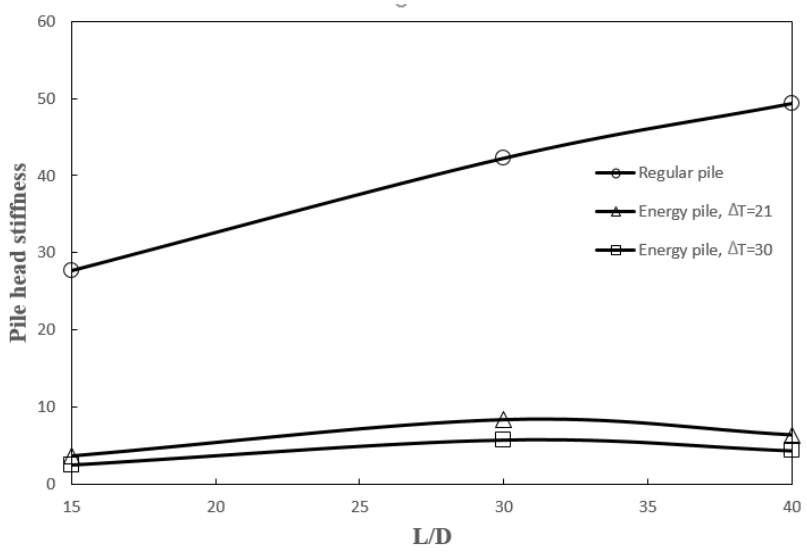

Figure 4.20. L/D versus pile head stiffness under the E-W component of the 2020 Izmir earthquake for the piles placed in clay

In Figure 4.19 and Figure 4.20, as the temperature increases the pile head stiffness reduces significantly, and the energy pile heated to 45^{o}C has the smallest pile head stiffness. The pile head stiffness of the regular pile increased as the L/D ratio increased. Heated piles did not show such a trend. Pile head stiffness increased when L/D ratio increased from 15 to 30; then it reduced from the L/D ratio of 30 to 40.

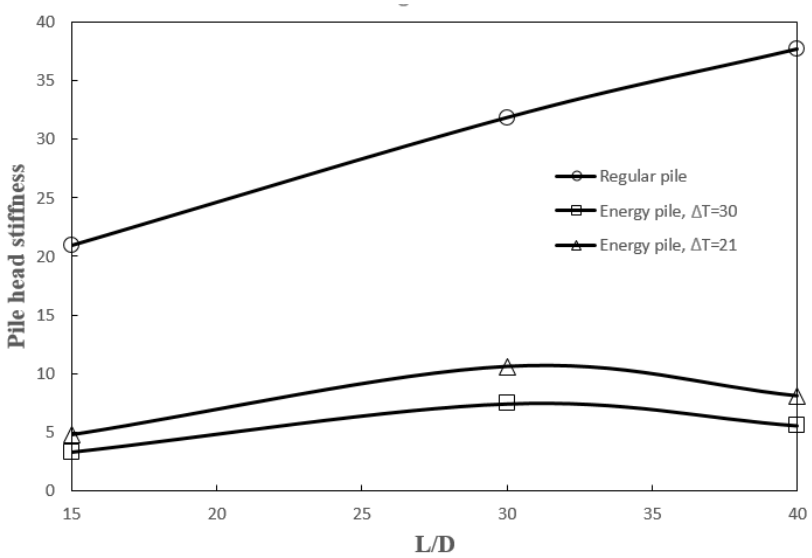

Figure 4.21. L/D versus pile head stiffness under the N-S component of the 2020 Izmir earthquake for the piles placed in sand

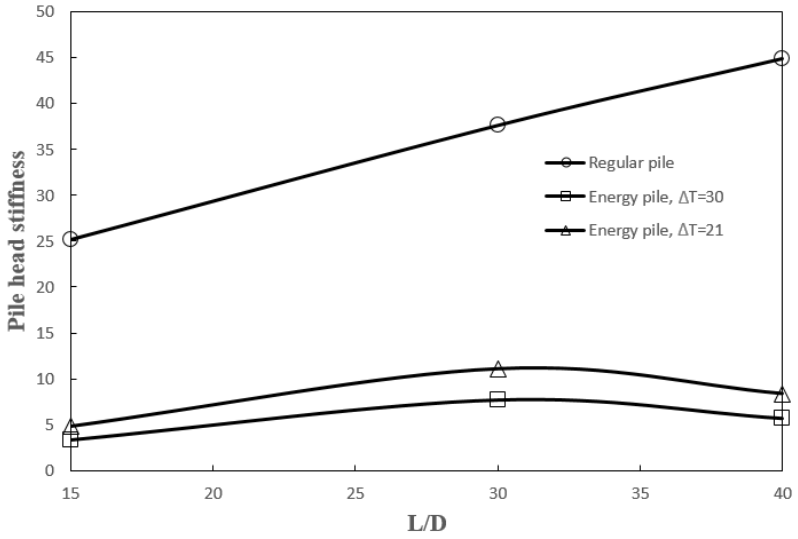

Figure 4.22. L/D versus pile head stiffness under the E-W component of the 2020 Izmir earthquake for the piles placed in sand

Same trend was observed in Figure 4.21 and Figure 4.22, the pile head stiffness of the regular pile increases with increasing L/D ratio, whereas the pile head stiffness of the energy piles increased when L/D ratio increased from 15 to 30, and it reduced from the L/D ratio of 30 to 40. This is attributed to the effects of geometric properties on temperature distribution, which affects the mechanical properties of the domain. Results from the piles placed in sand and clay showed that the pile head stiffness of the energy piles reduced significantly upon heating.

CHAPTER 5

CONCLUSIONS

In this thesis, earthquake response of axially loaded energy piles under temperature increases of 21ºC and 30ºC are investigated with L/D ratios of 15, 30, and 40 placed in cohesive and cohesionless soils, and the obtained results are compared with identical regular piles. Results showed a slight increase in energy piles due to heating in terms of acceleration and lateral displacement, while the steady-state temperature field was obtained. However, significant vertical displacements were observed. After the maximum pile head displacements were obtained, L/D versus pile head stiffness curves were generated. The conclusions of the work are summarized below:

- Acceleration and lateral displacement responses of energy piles were slightly increased, whereas the vertical displacement of the energy piles significantly increased under temperature rise. Since the pile was axially loaded prior to heating, it can be suggested that the effect of heating depends on the mechanical loading condition.
- Thermal expansion of soil under steady-state heating affects the magnitude and direction of vertical displacements because the higher values of soil thermal expansion coefficient increase the uplift effect on the pile head and seemingly provide a stiffer behavior upon heating.
- Geometric properties such as the L/D ratio affect the temperature distribution in soils.
- The difference in the response of energy piles and identical regular piles under N-S and E-W components of the 2020 Izmir earthquake indicates that there is also a possibility of a more drastic effect on the earthquake response of energy piles under different ground motions.
- Based on the findings of this thesis, the effect of heating on energy pile response must be considered in the design process. It is recommended that temperature dependency of soil parameters, including granular soils, must be investigated in sites where soil is exposed to thermal activities.

Future study on the topic can include a wide range of cases, such as:

- Effect of the groundwater table,
- Parametric studies such as:
  - ✓ Different initial soil elastic modulus values,
  - ✓ Different mechanical loading conditions,
  - ✓ Different soil thermal expansion coefficients which are greater, equal or smaller than that of pile thermal expansion coefficients,
  - ✓ Different ground surface temperatures and/or adiabatic ground surface assumptions,
  - ✓ Transient heat transfer with various temperature variations and durations including cooling.

These subjects may have a significant influence on the response of the energy piles, and there are also other essential parameters to expand the scope of this study and explore more about the response of energy piles under earthquake excitation.

REFERENCES

Abaqus 2012. Analysis User's Manual. Version 6.12, Dassault Systemes Simulia, Inc.

Abuel-Naga H. M., Bergado D. T., Lim B. F. 2007. "Effect of temperature on shear strength and yielding behavior of soft Bangkok clay", Soils and Foundations, 47(3), 423–436.

Abuel-Naga, H., Raouf, M. I. N., Raouf, A. M., & Nasser, A. G. 2015. "Energy piles: current state of knowledge and design challenges", Environmental Geotechnics, 2(4), 195-210.

Abu-Hamdeh, N. H. 2003. "Thermal Properties of Soils as affected by Density and Water Content", Biosystems Engineering, 86(1), 97-102.

Akrouch, G.A., Sánchez, M., & Briaud, J. 2014. Thermo-mechanical behavior of energy piles in high plasticity clays", Acta Geotechnica, 9, 399-412.

Alberdi-Pagola, M., Jensen, R. L., Madsen, S., & Poulsen, S. E. 2017. "Measurement of thermal properties of soil and concrete samples", Aalborg University. Department of Civil Engineering, DCE Technical Reports No. 235.

Amatya, B. L., Soga, K., Bourne-Webb, P. J., Amis, T., Laloui, L. 2012. "Thermo-mechanical behaviour of energy piles", Géotechnique, 62(6), 503–519.

Amis, T., Loveridge F. 2014. "Energy piles and other thermal foundations, developments in UK practice and research". REHVA Journal, 51(1), 32-35.

Arzanfudi, M.M. and Al-Khoury, R., 2018. "Freezing-thawing of porous media: An extended finite element approach for soil freezing and thawing". Advances in Water Resources 119, 210-226. https://doi.org/10.1016/j.advwatres.2018.07.013

Arzanfudi, M.M. and Al-Khoury, R. 2018. "Freezing-thawing of porous media: An extended finite element approach for soil freezing and thawing". Advances in Water Resources 119, 210-226. https://doi.org/10.1016/j.advwatres.2018.07.013

Arzanfudi, M. M., Al-Khoury, R., Sluys, L. J., Schreooers, G. M. A. 2020. "A thermo-hydro-mechanical model for energy piles under cyclic thermal loading", Computers and Geotechnics, 125, 1-18.

Bouazza, A., Adam, D., Singh, R. M., Ranjith, P. G. 2011. “Direct Geothermal Energy from Geostructures”. Australian Geothermal Energy Conference, 16-18 November, Melbourne, 245-248.

Bourne-Webb, P. J., Amatya, B., Soga, K., Amis, T., Davidson, C., Payne, P. 2009. “Energy pile test at Lambeth College, London: geotechnical and thermodynamic aspects of pile response to heat cycles”, Géotechnique, 59(3), 237–248. doi:10.1680/geot.2009.59.3.237

Bourne-Webb, P.J., Bodas Freitas, T.M., Assução, R.M. 2016. “Soil-pile thermal interactions in energy foundations”, Geotechnique, 66(2): 167-171.

Brandl, H. 2006. “Energy foundations and other thermo-active ground structures”, Géotechnique, 56(2), 81-122.

BS EN 1991-1-5:2003, Eurocode 1. Actions on structures. General actions. Thermal actions, BSI [Authority: The European Union Per Regulation 305/2011, Directive 98/34/EC, Directive 2004/18/EC] (Last access date: 07.09.2023).

Campanella, R. and Mitchell, J. 1968. “Influence of temperature on soil behavior.” J. Soil Mech. and Found. Div., 94, 709–734.

Cekerevac, C. & Laloui, L. 2004. “Experimental study of thermal effects on the mechanical behaviour of a clay”, International Journal for Numerical and Analytical Methods in Geomechanics, 28, 209–228. (DOI: 10.1002/nag.332)

Cekerevac, C. & Laloui, L. 2010. “Experimental analysis of the cyclic behaviour of kaolin at high temperature”. Géotechnique 60, No. 8, 651–655.

Das B.M. 2013. “Principles of geotechnical engineering”. 6th edn. Cengage Learning, Boston

Di Donna, A. & Laloui, L. 2015. “Response of soil subjected to thermal cyclic loading: experimental and constitutive study”, Engineering Geology, 190(1), 65–76.

Farouki, O. T. 1981. “Thermal properties of soils”. Hanover, NH: U.S. Army Corps of Engineers, Cold Regions Research and Engineering Laboratory.

François, B. and Laloui, L. 2008. “ACMEG-TS: A constitutive model for unsaturated soils under non-isothermal conditions”. International Journal for Numerical and Analytical Methods in Geomechanics, 32, 1955–1988.

Hamdhan, I. N., Clarke, B. G. 2010. “Determination of thermal conductivity of coarse and fine sand soils”, Proceedings of World Geothermal Congress, April 25-29, Bali, Indonesia, 1-7.

Hashash, Y. M., Phillips, C., Groholski. D. R. 2010 “Recent Advances in Non-Linear Site Response Analysis”, 5th International Conference on Recent Advances in Geotechnical Earthquake Engineering and Soil Dynamics, San Diego, California, 1-21.

Heidari, B., Garakani, A. A., Jozani, S. M., Tari, P. H. 2022. “Energy piles under lateral loading: Analytical and numerical investigations”, Renewable Energy, 182, 172-191.

Hudson, M., Idriss, I. M., and Beikae, M. 1994. “QUAD4M—A computer program to evaluate the seismic response of soil structures using finite element procedures and incorporating a compliant base”. Center for Geotechnical Modeling, Deptartment of Civil and Environmental Engineering, University of California, Davis, California.

Hussein, R. S., Albusoda, B. S. 2021. “Experimental and numerical analysis of laterally loaded pile subjected to earthquake loading”, Modern applications of geotechnical engineering and construction, Singapore, 291–303. doi: 10.1007/978-981-15-9399-4_25.

Khosravi, A., Moradshahi, A., McCartney, J., Kabiri, M. 2016. "Numerical analysis of energy piles under different boundary conditions and thermal loading cycles". E3S Web of Conferences. 9. 05005. 10.1051/e3sconf/20160905005.

Kömeç Mutlu, A., Mert Tuğsal, Ü. & Cambaz, M. 2023. “Zemin Hâkim Frekanslarının Farklı Algoritmalarla Belirlenmesi: İzmir Örneği”. Doğal Afetler ve Çevre Dergisi, 9(1), 58-70. DOI: 10.21324/dacd.1118207

Laguros, J. G. 1969. “Effect of temperature on some engineering properties of clay soils”. Highway research board special report (103), Conference on effects of temperature and heat on engineering behaviour of soils, Sponsored by The Committee on Physico-Chemical Phenomena in Soils, 186-193.

Laloui, L. 2001. “Thermo-mechanical behaviour of soils”, Revue Franc-aise de Ge´nie Civil, 5, 809–843.

Laloui, L. and Cekerevac, C. 2008. “Non-isothermal plasticity model for cyclic behaviour of soils.” International Journal for Numerical and Analytical Methods in Geomechanics, 32(5), 437–460.

Laloui, L. and Di Donna, A. 2011. “Understanding the behaviour of energy geo-structures”, Proceedings of the ICE–Civil. Engineering 2011; 164(4), 184–191.

Laloui, L., François, B. 2009. “ACMEG-T: Soil Thermoplasticity Model”, Journal of Engineering Mechanics, 135(9), 932–944.

Laloui, L., Nuth, M., Vulliet, L. 2006. “Experimental and numerical investigations of the behaviour of a heat exchanger pile”, International Journal for Numerical and Analytical Methods in Geomechanics, 30(8), 763–781.

Lysmer, J., and Kuhlemeyer, R. L. 1969. “Finite Dynamic Model for Infinite Media”, Journal of the Engineering Mechanics Division, 95(4), 859–877.

Marshall, A. 1972. “The thermal properties of concrete”, Building Science, 7, 167-174.

Martin, J.R., Abdelaziz, S. L., Olgun C. G. 2010. “Renewable Energy Applications Using Thermo-active Deep Foundations”, International Scientific Conference CIBv 2010, 12-13 November, Braşov, 289-304.

Maden Tetkik ve Arama Genel Müdürlüğü, Jeotermal Kaynaklar ve Uygulama Haritası, https://www.mta.gov.tr/v3.0/sayfalar/hizmetler/jeotermal-harita/images/3.jpg (Last access date: 15.09.2023).

Mitchell, J. K. 1969. “Temperature Effects on the Engineering Properties and Behavior of Soils”. Highway research board special report (103), Conference on effects of temperature and heat on engineering behaviour of soils, Sponsored by The Committee on Physico-Chemical Phenomena in Soils, 9-28.

Murayama, S. 1969. “Effect of temperature on elasticity of clays”, Highway Research Board Special Report (103), Conference on effects of temperature and heat on engineering behaviour of soils, Sponsored by The Committee on Physico-Chemical Phenomena in Soils, 194-203.

Olgun, C. G., Ozudogru, T. Y., Arson, C. F. 2014. “Thermo-mechanical radial expansion of heat exchanger piles and possible effects on contact pressures at pile–soil interface”, Geotechnique Letters, 4(3), 170-178.

Peron, H., Knellwolf, C., Laloui, L. 2011. “A Method for the Geotechnical Design of Heat Exchanger Piles”, Geo-Frontiers 2011: Advances in Geotechnical Engineering, GSP 2011, 470-479.

Rees, S. W., Adjali, M. H., Zhou, Z., Davies, M., Thomas, H. R. 2000. “Ground heat transfer effects on the thermal performance of earth-contact structures”, Renewable and Sustainable Energy Reviews, 4(3), 213–265.

Rotta Loria, A. F. and Laloui, L. 2016. “The interaction factor method forenergy pile groups.” Computers and Geotechnics, 80, 121-137.

Saggu, R., Chakraborty, T. 2015. “Cyclic Thermo-Mechanical Analysis of Energy Piles in Sand”, Geotechnical and Geological Engineering, 33, 321–342. https://doi.org/10.1007/s10706-014-9798-8

Salciarini, D., Ronchi, F., Cattoni, E., Tamagnini, C. 2015. “Thermomechanical effects induced by energy piles operation in a small piled raft”, International Journal of Geomechanics, 15(2): 1-14.

Suryatriyastuti, M. E., H. Mroueh, and S. Burlon. 2013. “Numerical analysis of the bearing capacity of thermoactive piles under cyclic axial loading.” Chapter 7 in Energy Geostructures: Innovation in Underground Engineering. Editors: Laloui, L., Di Donna, A. Hoboken, NJ: Wiley.

Suryatriyastuti, M., Burlon, S., Mroueh, H. 2016. “On the understanding of cyclic interaction mechanisms in an energy pile group”, International Journal for Numerical and Analytical Methods in Geomechanics, 40(1), 3–24.

T. C. İçişleri Bakanlığı Afet ve Acil Durum Yönetimi Başkanlığı, Deprem Dairesi Başkanlığı, Türkiye İvme Veritabanı ve Analiz Sistemi (AFAD-TADAS), https://tadas.afad.gov.tr/ (Last access date: 11.08.2023).

Tehrani, F. S., Salgado, R., Prezzi, M. 2016. “Analysis of axial loading of pile groups in multi-layered elastic soil”, International Journal of Geomechanics, 16(2), 1-18.

Tiwari, R., Jain, S., Chakraborty, T., Matsagar, V. 2012. “Dynamic response of reinforced concrete sacrificial walls under blast loading”. In: Proceedings of the 10th World Congress on Computational Mechanics (WCCM 2012), Sa˜o Paulo, Brazil, July 8–13.

Wang, W., Regueiro, R.A., McCartney, J.S. 2015. “Coupled Axisymmetric Thermo-Poro-Mechanical Finite Element Analysis of Energy Foundation Centrifuge Experiments in Partially Saturated Silt". Geotechnical and Geological Engineering, 33(2), 373–388.

Yavari, N., Tang, A. M., Pereira, J.-M., & Hassen, G. 2016. “Effect of temperature on the shear strength of soils and the soil–structure interface”. Canadian Geotechnical Journal, 53(7), 1186–1194.

Zienkiewicz, O., Emson, C., Bettess, P. 1983. “A Novel Boundary Infinite Element”, International Journal for Numerical Methods in Engineering, 19, 393–404.